Neural Circuit Mechanisms Underlying the Exacerbation of Alzheimer's Disease by Chronic Stress

TABLE OF CONTENTS

Acknowledgements	2
Glossary	3
Abstract	4
Introduction	5
Methods	30
Results	38
Discussion	46
Summary	57
References	58
Figures	73
Figure Legends	80

ACKNOWLEDGEMENTS

Firstly, I wish to thank the labs of William Klein (Northwestern University) and Karl Deisseroth (Stanford University) for their scientific collaboration; thanks also to Ivana Dellale (Boston University), Matthew Frosch (Massachusetts General Hospital), the Neuropathology Core of the Massachusetts Alzheimer Disease Research Center (P50 AG005134), and the Neuropathology Service of the Massachusetts General Hospital for their help in obtaining and processing human tissue samples. Though not included in this thesis, data from these experiments will likely contribute to any future manuscripts detailing the research herein.

Second, I wish to thank HHMI for facilitating and funding an exciting, rewarding, and formative one-year research fellowship. Special thanks to Melanie Daub and William R. Galey for their truly tireless work on behalf of the HHMI Medical Fellows.

Lastly and most importantly, to the Tsai lab – thank you for accepting me into a dynamic, creative, and incredibly productive group of scientists, and friends. I've found unending support and encouragement from all of you, but a few people deserve particular mention.

Li-Huei Tsai - your expectation for excellence was always balanced by guidance, and a solid confidence in my work. Through your advocacy, I never felt like anything less than a full member of the lab – an honor in itself. Thank you for giving me the opportunity to join your team.

Adam Bero – I often learned more from our coffee breaks than from hours of reading. Thank you for sharing your scholarship and principled approach to science.

Matthew Dobbin, Ram Magabushi, and Becky Canter – thank you all for your close instruction and guidance, and of course for all the humour.

Damien Rei – your mentorship and friendship has been paramount to any and all of my success in the Tsai lab. I hope that my year short with you has fulfilled the old proverb, that "shared joy is a double joy; shared sorrow is half a sorrow".

GLOSSARY

AAV_5:	Adeno-associated virus, serotype 5
Aβ:	Amyloid-beta
AD:	Alzheimer's disease
APP:	Amyloid precursor protein
BLA:	Basolateral amygdala (basolateral nuclear group)
CaMKII:	Calcium/calmodulin-dependent protein kinase
ChR2:	Channelrhodopsin-2
CNO:	Clozapine-N-oxide
CRF:	Corticotropin releasing factor
CRS:	Chronic restraint stress
CSF:	Cerebrospinal fluid
DG:	Dentate gyrus
eYFP:	Enhanced yellow fluorescent protein
GiDREADD:	Inhibitory G-protein-coupled "designer receptors exclusively activated by designer drugs"
GFAP:	Glial fibrillary acidic protein
GR:	Glucocorticoid receptor
HDAC2:	Histone deacetylase 2
JNK:	c-Jun N-terminal-kinase
HPA:	Hypothalamic pituitary adrenal (axis)
MCI:	Mild cognitive impairment
MR:	Mineralocorticoid receptor
NOL:	Novel object location
NOR:	Novel object recognition
PS1:	Presenilin-1
PS2:	Presenelin-2
PVN:	Paraventricular nucleus of the hypothalamus
RFS:	Repetitive foot-shock
RIP:	Regulated intramembrane proteolysis

ABSTRACT

Both epidemiological and animal studies have demonstrated a strong association between Alzheimer's disease (AD), neuropsychiatric symptoms such as depression and anxiety, and chronic psychological stress. The neurophysiological basis of fear, anxiety, and stress has been well studied and is thought to involve the basolateral amygdala (BLA) – a structure of the anterior temporal lobe, which interprets fearful stimuli and outputs a behavioral fear response. Similarly, dysfunction and maladaptation within limbic circuits involving the BLA is thought to be a common etiological factor of otherwise distinct neuropsychiatric disorders such as Major Depression, and Generalized Anxiety. To determine if increased BLA activity could act to accelerate the progression of AD, we manipulated a direct BLA-to-hippocampus circuit using optogenetic (ChR2) and pharmacogenetic (G_iDREADD) technologies, and subsequently examined hippocampal AD-related pathology, synaptic density, histone-deacetylase-2 expression, and hippocampus-dependent learning and memory abilities. We found that in wild-type mice, activation of glutamatergic BLA neurons was both necessary and sufficient to produce the molecular and cognitive effects of chronic stress. Terminal photostimulation of direct BLA afferents within the hippocampus was also sufficient, suggesting that the effects of chronic stress throughout the brain are mediated at least in part by direct excitatory projections originating in the BLA. Chronic activation of BLA glutamatergic neurons in the 5xFAD model of AD accelerated the neuropathological and cognitive AD-like phenotype, while chronic BLA inactivation had opposite effects. Overall our results suggest that neuropsychiatric disease and chronic stress may act through enhanced BLA activation to accelerate the progression of AD.

INTRODUCTION

Alzheimer's Disease as a Neuropsychiatric Disorder

Alzheimer's disease (AD) is a neurodegenerative disease of the cortical grey matter. It is the most common dementia in the United States (60-80 percent of all dementia cases, with a prevalence of 4.7-5.4 million), and is the sixth leading cause of death (1; 2). One in nine people older than age 65, and about one third of those older than 85 suffer from AD; as the population above age 85 increases through to 2050, the prevalence of AD is expected to climb to 13.8-16 million, accompanied by rising healthcare costs and public burden of disease (1; 2). Unfortunately there are currently few effective disease modifying treatments, and no available preventative therapy.

Although AD is a pathological diagnosis, the *Diagnostic and Statistical Manual of Mental Disorders V* outlines diagnostic clinical criteria for "probable" AD: *(i)* presence of a neurocognitive disorder, defined as decline in a cognitive domain (attention, executive functioning, learning and declarative memory, language, perceptual-motor, or social cognition) which interferes with independent functioning, *and (ii)* progressive gradual decline specifically in learning and declarative memory, *or* evidence of a Alzheimer's disease genetic mutation (3). Neuropsychiatric symptoms and affective dysregulation are also included in the symptom profile of AD (4).

New diagnostic guidelines from the National Institutes of Aging highlight the importance of biomarkers for the diagnosis of disease, which has lead to both a shift in research focus, and in perceptions of AD. "Pre-clinical AD" has been defined as a biomarker-positive but symptom-free stage, while precursory "mild-cognitive impairment" defines the earliest stages of cognitive decline

before frank dementia can be diagnosed (5). The symptomatic phase of AD is now thought to be the final result of years – and perhaps decades – of biochemical and neurophysiological derangement. These earlier changes produce the neuropathological hallmarks of this disease – Amyloid-Beta (Aβ) neuritic plaques and neurofibrillary tangles of hyperphosphorylated Tau protein (6). These two hallmarks also serve as the triggers of definitive diagnosis on autopsy, since clinical diagnosis is generally based on the exclusion of other causes of dementia (3). Although Aβ and Tau are well studied, the mechanisms of their toxicity, and thus the pathophysiology of AD, is largely unexplained. Two hypotheses have dominated the scientific literature over the past half-century: the cholinergic hypothesis, and the amyloid-cascade hypothesis (7) (8) (9).

Pathophysiology of Alzheimer's Disease:

The Cholinergic and Amyloid Cascade Hypotheses

Early hypotheses on the etiology of AD focused on the similarity with Parkinson's disease, in which neurodegeneration of the substantia nigra pars compacta leads to dopamine depletion and basal ganglia dysfunction. In the case of AD, another neuromodulatory neurotransmitter – acetylcholine – was postulated to be involved (9). The cholinergic nuclei project very broadly throughout the cortex and subcortical limbic structures, providing a powerful substrate for disease should these projections degenerate. Although cholinesterase inhibitors are indicated for the symptomatic treatment of AD (10; 11), metanalysis has demonstrated that these drugs have no effect on the rate of conversion from MCI to AD (12). Though circuit level dysfunction of the cholinergic system may contribute to attention and memory deficits in AD, the greater majority of evidence weighs in favor of another process being the *cause* of this disease.

The dominant hypothesis of AD pathophysiology is termed the "amyloid cascade". Briefly, cleavage of amyloid precursor protein (APP) – a ubiquitous transmembrane protein of unknown function – by membrane proteases produces short peptide fragments known as amyloid-beta (Aβ), which are thought to aggregate into neurotoxic oligomers and fibrillary polymers in the extracellular space (7).

Aβ generation begins with transport of APP to the cell membrane and axon terminal (13), where it associates closely with three membrane proteases – α-secretase, β-secretase (also known as β-amyloid cleaving enzyme, or BACE-1) , and γ-secretase (a multi-subunit complex composed of one of presenilin-1 (PS-1) or presenilin-2 (PS-2), and three accessory proteins) (14). Two divergent catabolic pathways of "regulated intramembrane proteolysis" (RIP) then proceed from this point. In the first pathway, APP is cleaved at the cell membrane first by α-secretase and then by γ-secretase, generating entirely soluble, "non-amyloidogenic" APP fragments (14). In the "amyloidogenic" pathway, APP is internalized to the endosomal fraction where it is cleaved first by β-secretase, then γ-secretase (15; 16). Exocytosis releases soluble fragments of either 40 ($A\beta_{40}$) or 42 ($A\beta_{42}$) amino acids in length, which self assemble into oligomers, protofibrils, and insoluble fibrillar plaques (15).

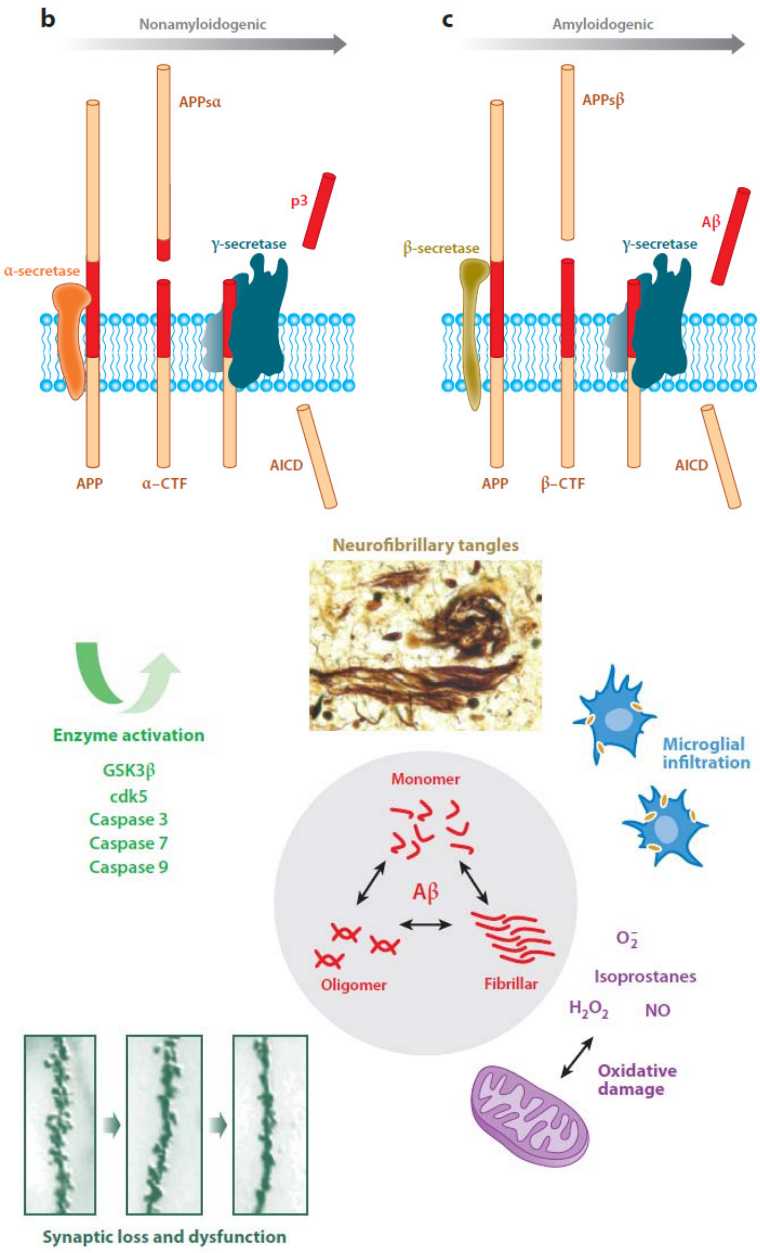

Introduction Schematic 1: APP cleavage Process (top panels) and general toxicity of polymerization (bottom panel). From O'Brien and Wong, 2011 (13).

The physiological function of APP remains unknown; APP knockout mice show no immediate phenotype, but may develop learning and memory deficits with age (17). Experiments *in vivo* and *in vitro* suggest that APP may act as a growth factor - regulating synaptic pruning, neuronal migration,

and neuron survival in development (18; 19). More recent studies offer more support to a hypothesized function in synaptogenesis and maintenance of synaptic density, but also provide evidence that APP may participate in calcium homeostasis, synaptic transmission, and epigenetic regulation of gene expression (through interactions with the histone acetyltransferase Tip60) (20). There is also work to suggest that Aβ fragments themselves may have a physiological function in decreasing activity at highly active synapses and facilitating LTP at low picomolar concentration, but most research on Aβ fragments has focused on direct neurotoxicity (21).

Evidence for toxicity of Aβ fibrils and oligomers is voluminous. Early work showed that a peptide fragment generated from APP and released into the extracellular medium was toxic to cultured hippocampal neurons (22). The neurotoxic effect of Aβ is increased in the presence of Tau protein, but the causality likely goes only one way: Aβ exposure alone leads to Tau hyper-phosphorylation, degeneration of the microtubule cytoskeleton, and neurite death (23; 24). Aβ exposure can also induce microglial activation, cause oxidative damage via mitochondrial dysfunction, generate apoptosis, or activate activity-dependent enzymes such as Cdk5 and Fyn-kinase, all of which may contribute to neuronal atrophy in AD (13; 25; 26). More recently, Aβ oligomers have been shown to bind with high affinity to cellular prion-protein at the post synaptic membrane (27; 26). This oligomer-prion-protein complex is capable of binding metabotropic receptors and directly activating intracellular kinases; blockage of this cascade ameliorates molecular and behavioral AD-like pathology in a mouse model (26). Furthermore, Aβ dimers isolated directly from post-mortem human tissue have been shown to impair long-term-potentiation, enhance long-term-depression, and cause loss of dendritic spines in hippocampal slice preparations (28).

The amyloid cascade hypothesis is also supported by genetic studies of early-onset familial AD, which is inherited in an autosomal-dominant fashion. 200 mutations in the genes encoding APP, PS1, and PS2 – all proteins in the APP catabolic pathway – have been associated with familial AD (29). Further genetic evidence for the role of APP and Aβ comes from patients with Down's syndrome (Trisomy 21), who carry an extra copy of the APP gene on the duplicate chromosome, and almost always develop AD-like pathology after age 40 (30). Deep sequencing studies of single-nucleotide polymorphisms on the APP gene has also identified a neuroprotective mutation that is found more frequently in the cognitively normal elderly population. This alanine-to-threonine substitution adjacent to the β-secretase cleavage site reduces the production of both $A\beta_{40}$ and $A\beta_{42}$, possibly facilitating the maintenance of normal cognition, and reducing AD incidence in carriers (31). Genome wide association studies have also implicated a number of proteins that may be involved in Aβ production, aggregation, and clearance through induction of inflammation (29). Finally, whole-genome sequencing studies have recently identified specific variants of two proteins - TREM2 and Phospholipase D3 - that are both associated with AD and also tied to Aβ processing (32–34). TREM2 is a surface receptor found on microglia, intimately tied to the regulation of neuroinflammation secondary to Aβ plaque formation, while Phospholipase D3 is a membrane-bound enzyme highly expressed by neurons of the hippocampus and limbic cortices, involved in APP processing and extracellular Aβ accumulation (34; 35).

Various mouse models have been developed based on the studies of AD genetics. The 5XFAD mouse carries a triply-mutated APP, and a human presenilin gene with two additional mutations.

This model uniquely develops dense $A\beta_{42}$ aggregates by two months of age with significant cognitive decline at six months (36). Because these mice lack abundant neurofibrillary tangle formation, neuronal atrophy, and cell death, the 5xFAD mouse is an especially useful model for preclinical AD. As no animal model has yet to recapitulate all aspects of AD pathology, the 5xFAD mouse is also a well-utilized model of AD in general (see methods for additional details).

Although the Aβ hypothesis has withstood twenty years of critical research, important questions remain. A significant number of patients without any cognitive decline show prominent dementia neuropathology, including amyloid angiopathy, lewy-bodies, and importantly Aβ plaques and neurofibrillary tangles throughout the hippocampus and cerebral cortex (37). Not surprisingly, the onset of cognitive decline correlates best with cerebral atrophy and synaptic loss, and the association between AD neuropathology and cognitive decline actually weakens as patients age, suggesting that plaque and tangle pathology may be a consequence (perhaps inevitable) of human brain aging (38). Recent metanalysis of 3500 independent cohort subjects with normal cognition has combined analysis of neuropathology, Aβ-ligand analysis by positron emission tomography, and CSF Aβ assays, concluding that the degree of amyloid burden accounts for approximately 12 percent of the variation in episodic memory, and 19 percent of the variation in global functioning. Although not diagnostically useful, this study supports the hypothesis that AD is a late result of a long-standing Aβ load. Indeed, one recent study (using a large cohort of patients with dominantly-inherited AD) examined the delay between appearance of biomarker changes in subjects and the age of AD onset in subject's parents. These authors found that declining CSF $A\beta_{42}$, and Aβ *deposition* in the precuneus (superior parietal lobe) are the earliest significant changes, detected 25 and 15 years respectively prior

to symptom onset (in the parents), followed by increased concentrations of CSF Tau and cerebral atrophy after an average delay of 5 years (see below) (39). The extended time frame of biochemical and neuropathological change following Aβ deposition suggests that early modulation of pathology – years or even decades before cognitive decline – could have symptomatic benefit.

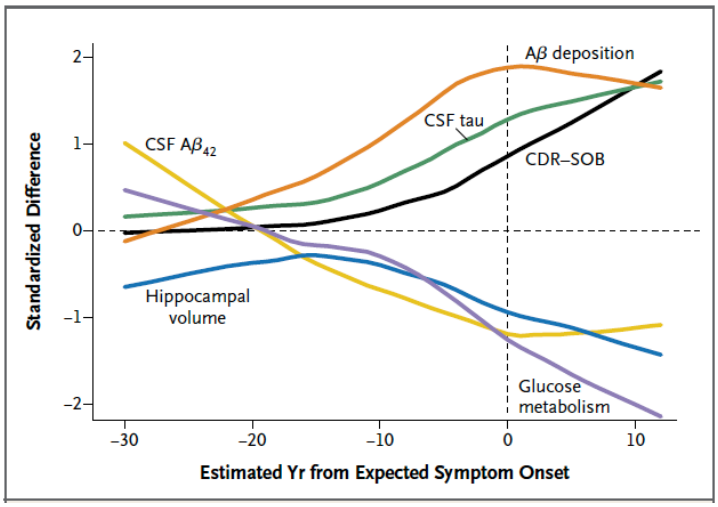

Introduction Schematic 2: Composite image from Bateman *et al.* (2012) demonstrating the chronology of pathological and biochemical changes in dominantly-inherited AD (39).

Previous studies from our lab have suggested that Aβ exposure may increase the expression of histone-deacetylase-2 (HDAC2) – a chromatin remodeling enzyme which is upregulated in both AD patients and AD mouse models, and likely contributes to disease pathogenesis and cognitive impairment in advanced AD (40). In otherwise healthy mice, over-expression of HDAC2 in neurons has been shown to impair spatial memory formation, reduce synaptic density, impair synaptic plasticity, and alter expression of a number of synapse associated genes (e.g. synaptophysin) (41). In vitro, exposure to Aβ increases HDAC2 expression by increasing glucocorticoid-receptor (GR)

phosphorylation, which enhances binding to the GR element on the HDAC2 promoter (40). Thus stress may be intimately tied to AD pathogenesis, and indeed there is much literature to support this hypothesis.

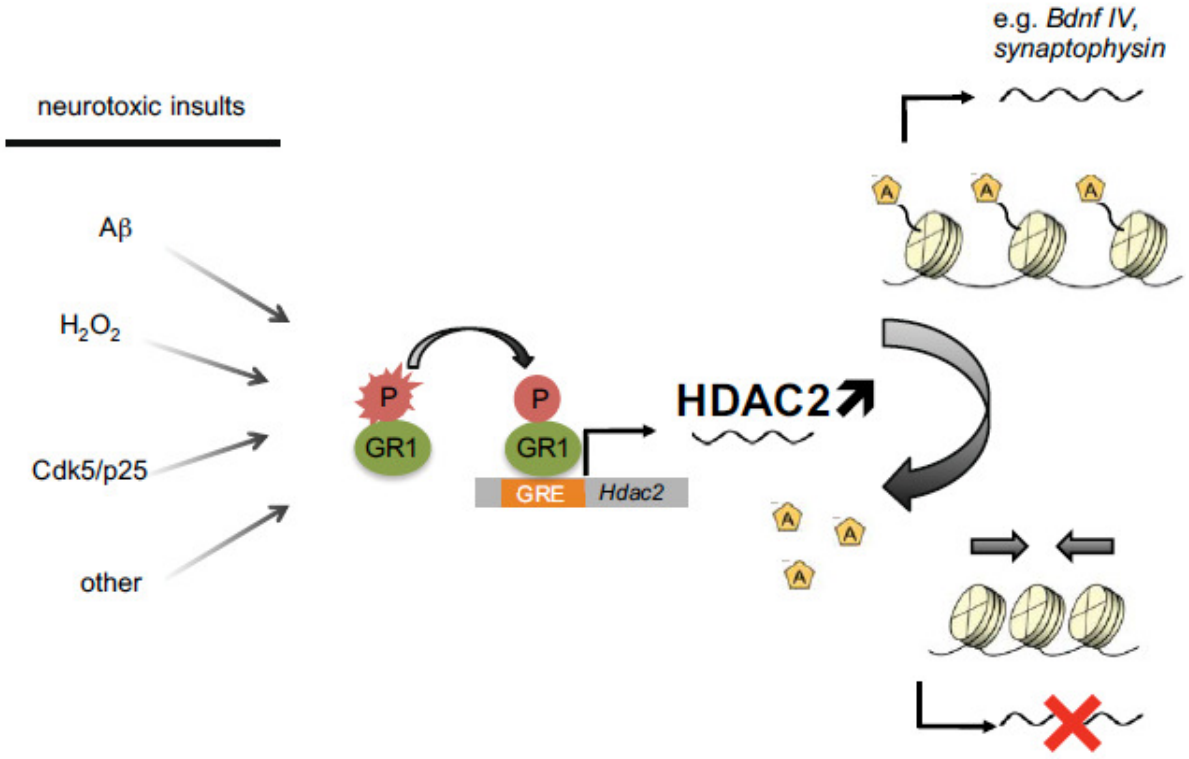

Introduction Schematic 3: From Graff *et al.* 2012, demonstrating a proposed pathway for stress-induced HDAC2 upregulation in neurodegeneration (40).

Neuropsychiatric Symptoms, AD, and Stress: Epidemiology and Human Studies

Epidemiology linking neuropsychiatric symptoms with AD is controversial. Although neuropsychiatric symptoms are commonly observed in AD, it has been difficult to determine if these are features of late-stage disease, prodromic symptoms, or genuine risk factors. Many cross sectional studies have concluded that neuropsychiatric symptoms – depression, apathy, agitation, and anxiety

for example – are common features of AD, and in fact have an overall prevalence approaching 90 percent on 5-year follow-up (42–44). Prospective studies using a measure called "distress proneness" (derived from the NEO Five-Factor Inventory of neuroticism (45)) were likewise able to demonstrate that patients who are prone to psychological distress are 2.4 times more likely to develop AD, and this trend persisted when patients with depressive symptoms were excluded (46).

Subsequent research has extended this result to show that distress proneness also increases the risk of developing MCI (47)(48). Indeed, a comprehensive review of 27 longitudinal and cross sectional studies estimates the prevalence of neuropsychiatric symptoms in MCI to 35-85%, and highlights the high frequency of depression, anxiety and irritability in these patients (49). Multiple groups have also conducted analyses to show that neuropsychiatric symptoms are not simply a characteristic of dementia – their presence is a risk factor for progression from MCI to AD (50–52)(53). Symptoms of anxiety were specifically implicated by one study (51), while two suggested that depression and apathy – features of major depression – were especially tied to progression (50)(52).

Consistent with the data on neuropsychiatric symptoms in general, comorbid Major Depression has been found to accelerate the rate of cognitive decline after the diagnosis of AD (54), and metanalysis has also shown that depression is a significant risk factor for the development of AD (odds ratio= 2.02) (55). The most recent cohort study found that the presence of Major Depression did not predispose a cognitively normal individual to developing MCI, but did find that once MCI was diagnosed, comorbid Major Depression increased rates of progression to AD (53). Post-mortem

neuropathological studies have also shown that patients with a history of major depression show increased plaque and tangle pathology (54).

Upwards of 65% of patients with major depressive disorders do not respond to the dexamethasone suppression test – that is, administration of a synthetic cortisol analogue fails to exert negative feedback on the hypothalamic-pituitary-adrenal (HPA) axis (56). This profound dysregulation of the HPA axis can also be observed in AD. AD patients frequently fail in the dexamethasone suppression test (57), show elevated salivary cortisol concentrations upon waking (58), and have an enhanced stress response following skin incision during surgery, as measured by plasma cortisol and epinephrine (59). Elevated cortisol may further exacerbate disease, as patients with elevated plasma cortisol experience more rapid cognitive decline (60), and a randomized controlled trial examining use of prednisone in AD showed a significantly more rapid cognitive decline with prednisone compared to placebo (61). Post-mortem studies of AD patients also demonstrate increased expression of Corticotropin Releasing Factor (CRF) – the trigger for cortisol release (see below) – in the hypothalamic paraventricular nucleus, suggesting that the central nervous system contributes to HPA overactivation in AD (62).

Thus data from both large populations and small samples of human patients demonstrate that distress, neuropsychiatric disturbance, and physical dysregulation of the stress response are all intimately tied to AD: these factors can predict the development of MCI, increase the likelihood of converting from MCI to AD, and accelerate the progression of AD once cognitive dysfunction has been established. The influence of prolonged stress on AD pathogenesis has not been directly

examined in human populations. However, results from animal models strongly support the hypothesis that stress has a profound effect on AD.

AD and Stress: Animal Models

Data from animal models has shown that chronic stress has the capacity to worsen disease-related pathology. The first study to demonstrate an effect of stress on AD pathology showed that social isolation reduced proliferation of neurons in the dentate gyrus of APP mutant mice (63). In double transgenic mice harboring human mutations in the APP and PS1 proteins, social isolation was found to increase Aβ production and impair memory through enhanced activation of the enzyme Cdk5 (64). Likewise, exposing 3xTg AD-model mice to altered social groups by mixing cage composition worsens the accumulation of neuritic plaques (65). In mice carrying an additional mutation in the Tau protein, intraperitoneal dexamethasone administration is able to increase Aβ accumulation, Tau-hyperphosphorylation and BACE-1 expression in a dose-dependent manner (66). This central effect is confusing given that dexamethsone has limited penetration through the blood brain barrier, and acts at the pituitary to suppress release of adrenocorticotropic hormone (67). Dexamethasone would however suppress the release of CRF, which then might carry forward to have central effects. Indeed, by using microdialysis to measure rapid changes in Aβ production, one recent study was able to determine that stress acted to exacerbate AD not through cortisol, but rather by increasing release of CRF which enhanced Aβ monomer production (68). Consistent with these observations, crosses of APP-transgenic mice with mice bred to overexpress CRF in the forebrain produces offspring with accelerated Aβ production and impaired cognition relative to APP-transgenics (69).

The Neurocircuitry of Stress and Memory

Stress is known to have a parabolic effect on cognitive abilities – acute stress can enhance memory and cognitive abilities while chronic unremitting stress has the opposite effect (70). Research into the effects of stress has focused on (1) the effects of glucocorticoids on CNS structures, in particular the hippocampus, and (2) direct effects of activating limbic circuits. Before discussing these two factors, it is necessary to introduce two major players: the hippocampus, and the amygdala.

The Hippocampus is perhaps the best-characterized structure in the mammalian brain, very likely because of the well-defined anatomical borders and histology, prominent size, and conservation across multiple mammalian species, all of which make it an easy target of curiosity. Anatomically, it is a structure of the medial temporal lobes bordered by the lateral ventricle superiorly, and continuous with the entorhinal cortex inferiorly (71). It can be functionally divided into the *dentate gyrus* (DG), *subiculum*, and *hippocampus proper* (also called *ammon's horn* in english, or *cornu ammonus* in latin) (71). The hippocampus proper can then be subdivided into 4 *cornu ammonus* (CA) fields in humans: CA1, CA2, CA3 and CA4 (72). The hippocampus proper can also be subdivided into various layers, or *strata* – one of which contains exclusively cell bodies (*stratum pyramidale*), while the others contain differing proportions of axons and dendrites, depending on the CA subfield (72)

The canonical circuit flow of information through the hippocampus begins with inputs from the entorhinal cortex, which project to cells of the dentate gyrus through the perforant pathway. These cells then project to the CA3 region via the "mossy fiber" axons, and the CA3 in turn projects to

CA1 via the "Shaffer collateral" pathway. CA1 cells project their axons to the subiculum, and these fibers coalesce to form the hippocampal fornix – the major output tract (72).

The study of the hippocampus in memory formation began with Henry Molaison, who had undergone bilateral medial temporal lobectomy which left him with a permanent anterograde and partial retrograde amnesia of declarative memory (73). The first characterization of long-term-potentiation, believed to be the neural correlate of memory formation, was also conducted in the hippocampus (74), and subsequent work has demonstrated a role for the hippocampus in the formation of episodic memory (75), and subsequent memory retrieval (76). The hippocampus is especially important in encoding spatial memory, and particular cells in the hippocampus (known as "place cells") will fire when an animal enters a defined location within a known environment (77). In addition to its role in memory formation, the hippocampus also functions as a limbic structure through its connections with the amygdala, cingulate gyrus and thalamus (71).

The Amygdala – named for its almond-like shape from the greek amygdálē– is a cluster of subcortical grey matter in the anterior temporal lobe. At the highest anatomical level, the amygdala can be divided into three divisions: the basolateral nuclear group (BLA), the centromedial nuclear group (CMA), and the superficial cortex-like nuclear group (SCLA) (78). These divisions are not only anatomical: the corticomedial group has a developmental history distinct from that of the basolateral group, and has even been relegated to status of "extended amygdala" by some classifications (79). *In vivo* diffusion tensor imaging of the human amygdala can also divide the structure along similar boundaries, suggesting that the organization of fiber tracts within the nuclei

(perhaps corresponding to dominant targets) segregates along with the three divisions that have been previously established (80). Lastly, fMRI analysis based on whole-brain connectivity and co-activation also divides the amygdala into highly similar groupings, suggesting that the previous cytoarchitectonic designations also accurately reflect separate functions (81). The *basolateral nuclear group*, (BLA) consists of three sub-nuclei: the *lateral nucleus, basolateral nucleus* (note to be confused with the *basolateral nuclear group* (BLA), which again includes all three sub-nuclei), and *basomedial nucleus* (78).

The response to stress involves both activation of the HPA, and of emotional circuits that facilitate the recognition of fearful stimuli, and a behavioral response.

HPA activation begins with release of the neuropeptide *corticotropin-releasing-factor* (CRF) by neurons in the paraventricular nucleus (PVN) of the hypothalamus (82). Although the canonical function of CRF is to promote the release of adrenocorticotropic hormone from the anterior pituitary, it is also centrally active as an excitatory neuropeptide, binding various G-protein coupled CRF receptors to increase cellular excitability (decrease threshold of excitability), and circuit activation (decreased seizure threshold) (83). CRF receptors are found throughout the limbic system including the hippocampus, and are especially dense throughout the BLA (84). BLA activation increases CRF release through excitatory connections to the PVN via the central and medial nuclei, suggesting a positive feedback loop (82) (85). The hippocampus, on the other hand, dampens the release of CRF through its connections with relay inhibitory neurons of the extended amygdala (85). Scattered and clustered CRF-positive neurons have also been found in the central nuclei of the

amygdala and in the CA1, CA3 and DG regions of the hippocampus, suggesting further capacity for circuit level regulation of CRF release by limbic structures such as the BLA and hippocampus (83).

The final downstream effect of CRF release from PVN neurons is cortisol release from the adrenal gland. Peripheral cortisol release has systemic effects that facilitate the stress response (ie, liberation of liver glycogen), but it also has effects on brain structures. Cortisol binds to both the high-affinity mineralocorticoid receptor (MR) and the lower affinity glucocorticoid receptor (GR), both of which are distributed in high density throughout the inhibitory feedback circuits of the limbic system, including the hippocampus (70). Cortisol binding has a "sweet spot" – both too little and too much can lead to dendritic debranching and impair cognition (70; 86).

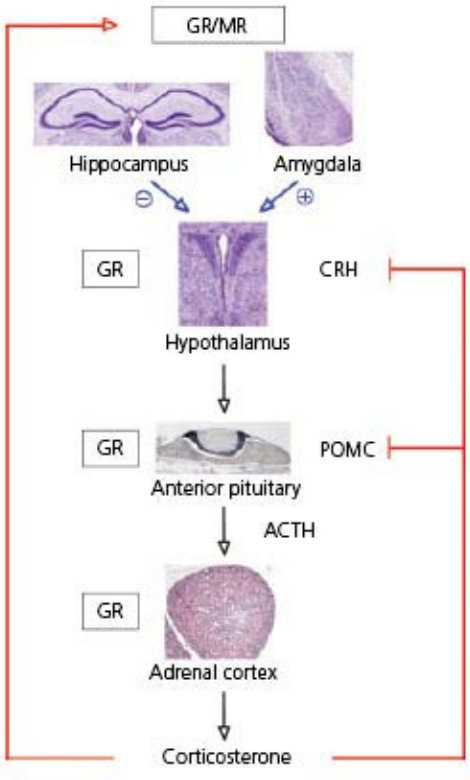

Introduction Schematic 4: Regulation of the HPA axis control by CNS structures (from Erdmann *et al.* 2008) (87)**. Abbreviations: CRH: Corticotropin Releasing-Hormone (or -Factor - CRF); GR: Glucocorticoid Receptor; MR: Mineralocorticoid Receptor; ACTH: Adrenocorticotropin Releasing Hormone; POMC: Pro-opiomelanocortin - an ACTH precursor.**

Circuits controlling the behavioral response to stress have been well-characterized using the fear-conditioning model, in which a subject (usually a rodent) learns to associate a particular environment with an aversive stimulus, like an electric shock (88). There is also good concordance between animal studies and neuroimaging studies in humans, suggesting that circuits controlling fear, anxiety and stress are well conserved (89).

Through this extremely expansive breadth of studies in both humans and animals, the amygdala has emerged as the most important structure in recognizing, responding to, and remembering fearful stimuli. Lesioning the BLA by injecting NMDA eliminates the expression of fear behavior in response to aversive stimulus (90). In humans exposed to a fearful stimulus, the right amygdala becomes activated only when a physiological response to the stimulus occurs, suggesting a function in association and expression of fear (91). Amygdala activation in response to fearful faces is also greater in healthy patients with high-anxiety states, suggesting an additional role for the amygdala in modifying and adapting fear behavior in response to emotional state (92). Amygdala activation is also important in the formation of emotional memory: when human subjects viewed emotional film clips, glucose metabolism in the right amygdala correlated with the subsequent memory of detail from the clips (93). This is consistent with animal studies showing that even long after exposure to a fearful stimulus, lesioning the amygdala reduces the recall of the fear memory (94). Finally, the amygdala is also a hub for the downstream activation of multiple limbic and cortical structures, including the anterior cingulate cortex, insular cortex, and hippocampus (95).

The flow of information through the amygdala has been well characterized. The lateral nucleus of the BLA receives multimodal external and internal sensory input, which are then integrated in the basolateral nucleus (For review, see Ledoux, 2000)(88). Neurons in the BLA then project directly and indirectly to the output nuclei of the CMA, and thus BLA activity can both promote and suppress anxiety, depending on the specific cell populations that become activated (96). The central nucleus of the amygdala then outputs to various regions to drive the behavioral response to fearful stimuli (97). For example, specific projections to the hypothalamus, parabrachial nucleus and ventral

tegmental area mediate the risk avoidance, respiratory response, and emotional valence of fear, respectively (98). However, the BLA also projects directly to the hippocampus, which will be discussed in detail below.

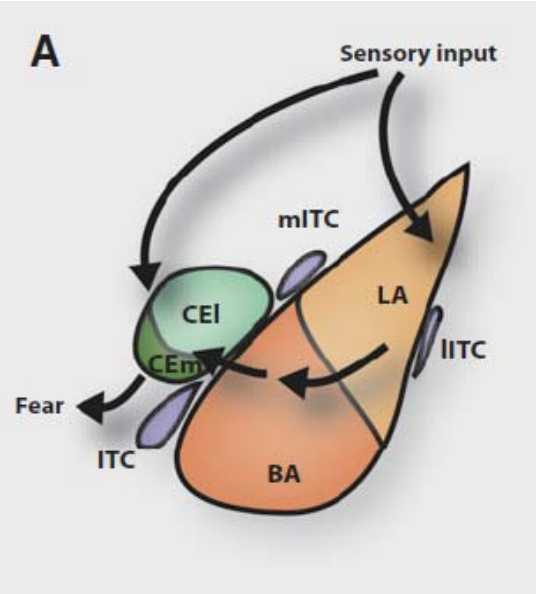

Introduction Schematic 5: General flow of information through the amygdala. From Ehrlich *et al.* 2009 (99). **Abbreviations: BA: Basolateral nucleus of the Basolateral Nuclear Complex; LA: Lateral nucleus of the Basolateral Nuclear Complex; CEl: Lateral subdivision of the Central Nulceus; CEm: Medial Subdivision of the Central Nucleus; ITC: Intercalated cell cluster**

The function of the amygdala as a neural integrator is so strong that only 4-7 percent of amygdala neurons will respond to unimodal sensory stimulus (gustatory, visual, olfactory), whereas complex stimuli such as an expressive face or accelerating heartbeat elicit strong action potential responses from excitatory amygdala projections (78). At a structural level, imaging studies also demonstrate amygdala response to emotional pictures, and emotional faces (for review, see Shin, 2010)(89).

In states of acute stress, the BLA enhances memory formation through connections with memory structures such as the hippocampus (100; 101). For example, infusion of the noradrenergic agonist clenbuterol into the BLA during behavioral training enhanced memory recall and hippocampal expression of the immediate-early-gene *Arc,* suggesting the BLA can modulate hippocampal activity (102). Lesions of the BLA block the memory facilitation induced by glucocorticoid infusion into the hippocampus, and likewise block the memory impairment induced by either adrenalectomy or intra-hippocampal infusions of a GR antagonist (100).

While acute stress generally enhances memory formation, chronic stress has the opposite effect (70; 103). At a cellular level, chronic stress leads to contrasting patterns of dendritic remodelling in the BLA and hippocampus: elaboration of dendritic arborisation occurs in excitatory projection neurons of the BLA, while debranching and regression of apical dendrites occurs in CA3 pyramidal neurons following chronic stress (70; 104; 105). Indeed, this dendritic remodelling of the BLA following chronic stress has been shown to increase baseline excitability of regional neurons, suggesting that BLA output may be increased in states of chronic stress (105).

Thus many studies suggest that the BLA participates in neurophysiological changes associated with stress. Unknown however, is whether the direct circuit connectivity between the BLA and associated structures (such as the hippocampus) facilitates these changes, or rather if some secondary factor such as HPA axis activation is responsible.

Circuits Linking Stress and Cognition

The hippocampus is both physically adjacent to the BLA, and functionally integrated in providing emotional content to memory. Even considering the confusing, often impenetrably dense, and sometimes contradictory nomenclature of amygdala anatomy, trends emerge from studies in both rodents and non human primates that sketches an extensive network of monosynaptic connections between these two structures.

There is extensive reciprocal innervation of the BLA (lateral, basolateral and basomedial subnuclei), and all hippocampal subfields, except notably the DG which neither receives nor sends any projections to the BLA (106–108). First, in the rat (*Rattus norvegicus*) all three subnuclei of the BLA send projections most densely to the ventral ("temporal") two-thirds of the hippocampus. In the rat, projections to CA3 originate in the basolateral subnuclei exclusively; projections to hippocampal CA1 and the subiculum seem to be segregated by cell layer: the strata molecular and lacunosum (internal axonal layers) receive input from the basomedial nucleus, while the strata oriens and radiatum (external, dendritic layers) receive from the basolateral nucleus (109). In rodents the temporal CA1 was observed to receive more connections from all BLA subnuclei, and is the only hippocampal subfield to send reciprocal afferents back to the BLA (108). The interconnections between the BLA and entorhinal and perirhinal cortexes are interesting in their capacity to modify and modulate hippocampal output, but are beyond the scope of this discussion.

In the rhesus monkey (*Macaca mulatta*) as in the rat, BLA afferents to the hippocampus consistently originate in only the basolateral and basomedial subnuclei of the BLA, and their projections form a

more dense "continuous band" throughout the hippocampal subfields (106; 107). In contrast, projections from the lateral subnuclei of the BLA are sparse, as are those from all of the centromedial and cortical nuclei (106). CA4 through CA1 receive inputs from the basomedial nucleus, while the prosubiculum and subiculum receive their projections from the parvocellular division of the basolateral subnucleus (107). Unlike in the rat, amygdala projections in primates terminate most often in the dorsal ("septal") hippocampus (106). Reciprocal connections from the hippocampus originate most often in dorsal CA1 – these *do not travel via the fornix*, but instead via a direct tract through the angular gyrus known as the "angular bundle" (106). Reciprocal hippocampal afferents terminate in all BLA subnuclei according to Aggleton (1986), or exclusively in the basolateral and basomedial subnuclei according to Saunders (1988).

These studies show interesting commonalities – that the BLA, and perhaps specifically the basolateral and basomedial subnuclei, are especially reciprocally connected with the hippocampus CA1. This suggests a conserved organization to amygdala-hippocampus connectivity, which can be manipulated experimentally or therapeutically to examine the effect of stress on memory and AD.

Amygdala (Dys)Function in Disease

Psychiatric disease suffers from a symptom-based classification system that bypasses structural, chemical, and genetic etiologies. Thus, multiple psychiatric conditions can share contributing pathophysiology. For example in both Major Depressive disorder (110), and Anxiety-disorders (111), there is enhanced activation of the amygdala in response to presentation of a fearful face. Treatment of depression with Citalopram (a selective serotonin reuptake inhibitor) normalizes the

response of the amygdala to fearful faces after only seven days – an interesting result considering that full symptomatic relief generally occurs only after weeks or months of treatment (112). Beyond these changes in amygdala activation, psychiatric disease also features changes in the functional connectivity of the amygdala with other brain regions. As measured by correlations in metabolic activity (Fludeoxyglucose (F18) Positron Emission Tomography [FDG-PET]), patients with bipolar disorder demonstrate stronger connectivity with the prefrontal cortex and hippocampus; in unipolar depression there is also a stronger, though negative, connectivity with prefrontal cortex (113). Dysfunction of amygdalar circuitry might thus contribute to multiple classes of psychiatric disorders.

In AD, epidemiological literature suggests that neuropsychiatric symptoms are present before memory disturbance, and contribute to disease progression (see above). However, it is possible that instead, amygdalar changes are *secondary* to AD-related degeneration, and themselves lead to limbic dysfunction and neuropsychiatric symptoms. Indeed the amygdala has been shown to lose functional connectivity with the both the hippocampus and various frontal cortical regions in AD (by resting state MRI analysis), and these changes correlate with clinical assessments of cognitive status (114). There is also morphometric evidence to suggest that amygdalar degeneration correlates with cognitive decline in AD. For example, one recent structural MRI study demonstrated a correlation between recall of emotionally charged words and gray matter volume of the amygdala and hippocampus (after normalization for overall cortical volume), while another found a similar association between emotional memory abilities and amygdalar (but not hippocampal) volumes (115; 116). Regarding neuropsychiatric symptoms in particular, although one study found a trend suggesting that AD patients who experienced clinical anxiety showed relative preservation of the

amygdala from degeneration (117), the bulk of evidence speaks *against* a specific correlation between amygdalar degeneration or preservation in AD, and presence of neuropsychiatric symptoms (118). Overall these studies suggest that although amygdalar dysfunction contributes to cognitive decline in AD, it does not obviously relate to the presence or absence of neuropsychiatric symptoms. However, the importance of chronic amygdala activation to overall disease progression (as is suggested by the epidemiological link between AD and long standing "distress") has not yet been addressed.

FOCUS OF THE CURRENT STUDY:

To summarize, AD is a disease in which emotional dysregulation and neuropsychiatric symptoms are common. The pathophysiology of AD is well understood to involve Aβ and Tau-induced derangements in neuronal function, and eventually neuronal atrophy and death. Animal models have established a link between chronic stress, and exacerbation of these pathological hallmarks of disease; the epidemiological literature has provided an equally strong link between stress, neuropsychiatric symptoms, and accelerated AD progression or increased incidence. The BLA is known to underlie many of the effects of stress, and also known to be dysfunctional in multiple neuropsychiatric disorders. Perhaps then, multiple neuropsychiatric symptoms converge to act on a common structure – the BLA – and increased activity of this structure accelerates AD. The experiments outlined below seek to assess two hypotheses: (1) that direct BLA-to-hippocampus circuit activity underlies the cognitive and molecular effects of chronic stress, at least in the domain of spatial memory and (2) that directly manipulating this sensitive circuit can alter pathological progression in the 5xFAD mouse model of AD.

To address these hypotheses, we used optogenetic and pharmacogenetic strategies to specifically manipulate excitatory projection neurons of the BLA. Intraparenchymal injection of adeno-associated virus (AAV_5) encoding channelrhodopsin-2 (ChR2) allowed us to examine structural activation (96; 119; 120), while injection of virus encoding GiDREADD enabled us to examine structural inactivation (121–123) (see fig. 1 for a summary of experimental paradigms). Briefly, we found that the activity of glutamatergic cells of the BLA was (1) necessary for chronic-stress induced molecular and cognitive changes (2) sufficient to replicate these changes in the absence of any stressor. We also found that direct and selective activation of only BLA terminals arriving in the dorsal hippocampus was sufficient to replicate these effects. In the 5xFAD model of AD, we replicated previous findings that chronic stress exacerbated AD pathology. Applying our earlier results to the 5xFAD model, we found that chronic BLA activation could worsen AD pathology and impair cognition, while chronic inactivation slowed pathological progression, and may improve cognitive function.

METHODS

Animals

All mouse work was approved by the Committee for Animal Care of the Division of Comparative Medicine at the Massachusetts Institute of Technology. Adult male Swiss Webster mice (Taconic, Charles River) were caged in groups of 4 to 5 on a normal light dark schedule and given access to food and water *ad libitum.* 5xFAD homozygote mice in a B6SJL genetic background were obtained from The Jackson Laboratory. These mice express human APP harboring the Swedish, Florida, and London Familial-AD mutations, and human Presenilin-1 harboring the M146L and L286V Familial-AD mutations, all driven by the neuron-specific promoter *Thy1*. In the 5xFAD mouse, extraneuronal amyloid deposition begins at 2 months (preceded by intraneuronal accumulation), with significant loss of synaptic density and layer-5 cortical pyramidal neurons by 9 months (trend at 4 months), and increase p25 by 9 months (36). All mice were used at an age of 3 months for the RFS treatment, 10 weeks for the BLA-cell body viral injection (to allow 3 weeks for viral expression) and 8 weeks for the BLA-terminal viral injection (to allow 6 weeks for viral expression).

Repetitive Foot Shock (RFS)

Mice were placed in fear conditioning chambers (TSE systems) for 1 hour between 10 AM and 6 PM. Freezing and behavioral activity was automatically measured using TSE fear conditioning software. Mice received 10-foot shocks at an intensity of 0.8mA and at random intervals during a one-hour session. Control mice were placed in the chamber for 1 hour but did not receive foot shocks. This procedure was repeated for 7 days.

Chronic Restraint Stress (CRS)

Each CRS session began at a variable time, between 10:00 AM and 6:00 PM. Plastic DecapiCones (Braintree Scientific) were prepared by cutting 5 mm from the small open end to allow for easier breathing, and a large hole near the tail for excreta. The cone was secured around the tail using elastic bands or labeling tape. Mice were arranged in the bottom of a large rat cage on a lab bench, and inclined to allow for urine and feces to clear from the bags. CRS sessions lasted 2 hours, after which mice were quickly returned to their home cage. Control mice were brought to the lab bench but left in their home cages for 2 hours.

Surgeries

All surgeries were performed under aseptic conditions (with stereotaxic guidance for intracranial injections). Mice were anesthetized using 1 to 2% isoflurane and Ketamine/Xylazine. All coordinates are relative to bregma in mm and defined according to the Paxinos sterotaxic atlas (124).

G_iDREADD – All mice received bilateral injections of adeno-associated virus (AAV_5) virus (1-$5*10^{12}$) expressing Gi-DREADD under the CaMKIIα promoter (http://genetherapy.unc.edu/services.htm#AAV). Virus was provided by the UNC vector core. Swiss-Webster mice received a bilateral injection of 0.5 µl at a rate of 0.05µl/min using 10µl elongated glass capillary (Wiretrol Drummond) and a microinjector (Quintessential Steroetaxic Injector, #53311); 5xFAD mice received a bilateral injection of 0.3 µl at a rate of 0.05µl/min using the same equipment. Stereotaxic coordinates for BLA injections in Swiss Webster mice were (-1.34 mm AP, ±3.35 mm ML, -3.9 mm DV) and in 5xFAD mice were (-1.14 mm AP ±3.51 mm ML, -3.9mmDV). After injection, the capillary was left in place for an additional 5-10 minutes to allow

for virus diffusion, and then was slowly withdrawn. Animals were kept on a 37° heating pad during the surgery, and until recovery from anesthesia.

The Gi-DREADD activating drug Clozapine N-oxide (Sigma Aldrich, C0832) was diluted in 0.9% sterile saline (Aqualite System) and injected i.p. (2.5mg/kg) 30 minutes prior to starting the RFS treatment. For osmotic pump delivery, CNO was diluted in 0.9% sterile saline to a concentration of 5mg/mL. Approximately 240 µL of CNO solution was loaded into the Alzet® model 2004 pump. The pump was implanted subcutaneously using a 1cm dorsal incision made at the base of the neck between the scapulae.

ChR2 – Intracranial injections were performed as described in the **G_iDREADD** section. Control of BLA glutamatergic projection neurons was achieved using an AAV_5 vector carrying hChR2(H134R)-eYFP , or control virus carrying eYFP only, both driven by the CaMKIIα promoter (viruses provided by Karl Deisseroth, maps and clones available at http:// www.optogenetics.org). All mice were bilaterally implanted with self assembled implantable optical fibers using the protocol from the synthetic neurobiology website (http://syntheticneurobiology.org/protocols/protocoldetail/35/9), with the only difference being the use of metal ferrules with an internal diameter of 330 µm (precision fiber products) and 300 µm fiber optic, 0.37 NA (Thorlabs). For ChR2-cell body mice the implants were placed 0.5mm dorsal to the BLA (Swiss Webster: (-1.34 mm AP, ±3.35 mm ML, -3.4 mm DV) 5xFAD: (-1.14 mm AP, ±3.51, -3.4 mm DV)). For the ChR2-terminal experiments, implants were placed 0.5mm dorsal to the hippocampus CA3 in the dorsal hippocampus (-2.18 mm AP, ±2.67 mm ML, -1.37 mm DV). Two self-tapping bone screws (Bioanalytical Systems) were screwed into the scull to hold the implant in place. One layer of adhesive cement (C&B metabond;

Parkell, Edgewood, NY) followed by cranioplastic cement (Dental cement; Stoelting, Wood Dale, IL) was applied to the implants, skull, and screws to secure these elements to the skull. Virus was allowed to express for 3 or 6 weeks for the cell body or terminal experiments respectively, before beginning the laser stimulation paradigms.

Optogenetic Stimulation

A fiber-optic cable was used to connect a 473 nm laser diode (OEM Laser Systems, East Lansing, MI) through an FC/PC adapter to a rotatory joint (Doric Lenses) mounted inside the fear-conditioning chamber (TSE Systems). Laser output was controlled using a Master-8 pulse stimulator (A.M.P.I., Jerusalem, Israel). All included animals had the center of the viral injection located in the BLA, though there was occasional leak to neighboring regions or along the needle tract. Specificity of the stimulation was dependent on fiber optic implant location, and was histologically confirmed in all cases. The skull-mounted optical fibers were plugged to a branching fiberoptic patchcord (Doric Lenses) to split the laser output, providing bilateral light delivery. This patchcord was connected to the external fiber optic cable through the rotatory joint inside the fear-conditioning chamber. Once connected, mice were allowed 3 min to acclimatize before starting the laser stimulation. BLA-cell body photostimulation in Swiss-Webster mice consisted of pairing 4.5-kHz tone pips (1 Hz; 250 ms on/ 750 ms off) for 20 s with 2 s of laser stimulation (20 Hz; 10 ms pulse-width; 473 nm; 3-5 mW; ~57 mW/mm^2), which coterminated with the tone, occurring 16 times during a 20 min period at variable interval, repeated daily for 7 days. Terminal photostimulation in Swiss Webster mice consisted of either an identical paradigm to that for cell body stimulation, or 20s of constant laser stimulation at 7-8 mW (~106 mW/ mm^2 at the tip of the fiber) occurring 10 times during a 20 min session at random intervals, repeated daily for 7 days. BLA-cell body photostimulation in 5xFAD

mice consisted of 20 sec of laser stimulation (20 Hz; 5 ms pulse-width; 473 nm; 1-3 mW; ~34mW/mm^2) occurring 10 times during a 20 min session, repeated daily for 14 days.

Behavioral assays

Novel Object Recognition/Novel Location Recognition – Behavioral arenas consisted of 4 rectangular rat cages with no bedding, arranged in a 2x2 rectangle, separated by four opaque walls. A triangle or three vertical lines of red labeling tape were placed onto the two opposing short walls for spatial cues. For novel object recognition and novel object location, mice were placed into the arenas on day 5 and 6 of the RFS or laser-stimulation paradigm, and allowed to explore and familiarize for one 10 min session per day. On day 7, the novel object location protocol started with the training phase, wherein two objects were placed along one short side of each arena (100ml Pyrex glass bottles, positioned in the corners, 3 cm away from the walls). The mice were placed facing the middle of the opposite short wall at its midsection. Mice were allowed to familiarize with the objects for two 10 min training sessions, separated by an inter-trial interval of 1h. 75 min after the second training session, one of the objects was moved to the opposite corner and mice were again placed into the arenas. Immediately following this testing period, the novel object recognition procedure started with the training phase, in which the two objects were placed in their original location and mice were allowed 10 additional min of free exploration. 24h later, one of the glass bottles was substituted for a plastic 55ml bottle and the mice were again placed into the arena. For both tests, time spent with each object (old and new locations or old and new objects) was recorded during a 5 min testing period. During each step of the training and testing, video of the performing mice was acquired using a Sony Camcorder fixed to the ceiling above the arenas. Videos were analyzed by an experimenter blind to the experimental treatment. Mice were scored as exploring an object if they

showed obvious signs of directed attention: climbing, sniffing, or prolonged observation (if within approximately 2 cm of the object). Time spent on top of the objects was not counted, unless the mice were simultaneously directing attention to the object.

Fear Conditioning – Mice were allowed to habituate to the fear-conditioning room for at least 30 minutes prior to starting the procedure. The fear conditioning chambers (TSE) were scented using a paper towel saturated with natural vanilla extract. Background noise was set to 0.1 dB. Mice were given 3 minutes to habituate to the box. Two 0.8 mA shocks were administered, each preceded by a 30 seconds of 4.5 kHz tone pips. 15 seconds after the final shock, mice were returned to the home cage. Boxes were disinfected with quatricide between mice, and the paper towel was re-saturated with vanilla. 24 hours later, mice were returned to the unaltered chamber and freezing was assessed for 3 minutes (no tone, no shock). After contextual testing, the boxes were cleaned and modified: the vanilla extract was replaced with 2 % Acetic Acid, the metal shock bars were covered with a grey plastic flooring, the walls of the box were covered with yellow paper, and the background noise was removed. Mice were then returned to the box for cued testing and freezing was assessed during 3 minutes of constant 4.5 kHz tone pips.

Immunohistochemistry

Mice were perfused with 10% paraformaldehyde under deep anaesthesia (ketamine, xylazine) and their brains sectioned at 40 μm thickness using a vibratome (Leica). Slices were permeabilized with 0.1% Triton X-100, blocked (10% donkey serum), and incubated overnight with 0.1% Triton X-100/10% donkey serum in PBS containing primary antibodies: rabbit HDAC2 (Abcam; 1:1000), Mouse synaptophysin (Sigma; 1:1000), Rabbit GFAP (Abcam; 1:10,000), Mouse 4G8 (Covance, 1:500), and Mouse Nu-1 (William Klein, Northwestern University; 1:3600). Primary antibodies

were visualized with Alexa-Fluor 488, Cy3 and Cy5 antibodies (Molecular Probes), and neuronal nuclei visualized with Hoechst 33342 (Invitrogen). Images were acquired using a confocal microscope (LSM 510, Zeiss; LSM 710, Zeiss) at identical settings and focal plane for each of the conditions. Images were quantified using ImageJ 1.42q by an experimenter blind to the experimental treatment. For HDAC2 and SYP quantification, sections at bregma -1.70 were selected and 5 images per section were acquired. For HDAC2 40-60 representative cells were analyzed, while for SYP, the *stratum radiatum* region of the CA1 subfield was selected in each picture and the mean intensity was quantified. For GFAP, a similar protocol was used with the exception that all *strata* were analyzed. For 4G8 plaque load analysis, two sections at bregma -2.18 were analyzed under epifluorescence by a blinded experimenter. 4G8-positive plaques were counted in the DG, and CA1. Aggregates were determined to be individual plaques if their total size was larger than a nuclei, and if they could be resolved from adjacent aggregates. For Nu-1 analysis, 2 sections at bregma -2.18 were selected. A single image of the DG and septal CA1 was acquired for each hemisection with identical settings and focal plane. Images were exported to ImageJ 1.42q, thresholded for intensity, converted to binary, and finally the percent coverage of all *strata* **except** the *stratum pyramidale* was calculated based on a constant threshold intensity.

Corticosterone Assays

Following the fifth session of RFS/optogenetic stimulation or the final session of CRS, mice were scruffed, and the facial vein was punctured within 5-10 seconds using a 5 mm Goldenrod Animal Lancet (MEDIpoint). 5 drops of blood were collected on ice and heparinized with 10 µL of 1000U/mL heparin. Samples were centrifuged at 4000 RPM for 10 minutes at 4°C, the plasma removed, and frozen for later use. A corticosterone ELISA kit (Enzo Life Sciences) was used to

measure concentration of these samples. The provided steroid displacement reagent was mixed with assay buffer, and this mixture was used to dilute the plasma samples to the suggested ratio of 1:50, and such that 2.5 parts steroid displacement reagent were present for every 97.5 parts undiluted sample. The rest of the protocol was conducted as per the manufacturer's instructions. Absorbance at 405 nm was read using a multiplate reader (EnSpire; PerkinElmer), blanked to blank-wells. Concentration was calculated from the standard-curve provided by standard concentration in each plate.

Statistics

Statistical analyses were performed using GraphPad Prism 5. One-way analyses of variance followed by Tukey post-hoc tests, one-tailed Student's *t*-tests, and the Pearson product-moment correlation coefficient were used unless otherwise indicated. All data are represented as mean±s.e.m. Statistical significance was set at $P \leq 0.05$.

RESULTS

In experiments begun by a postdoctoral fellow and continued in collaboration, we first sought out to characterize the effects of chronic stress on hippocampus-dependent cognition and hippocampal synaptic density, by subjecting Swiss-Webster mice to 7 days of either "repetitive inescapable footshock" (RFS), or context-only control treatment (Fig. 1a). Cognitive testing on the final two days of this paradigm revealed deficits in low-stress, hippocampus-dependent memory tasks: mice showed no preference in the novel-object recognition (NOR) task measured at 24 hours (Fig 2a, t-test, P=0.0079, n=10,16), and no preference in the novel-location-recognition (NLR) task measured at 1 hour (Fig. 2a, t-test, P<0.0265, n=10/group). As control measures, total displacement, velocity, and exploration time were not significantly different between the control and RFS-treated groups during the NOL task (Appendix Fig.1 c-e). After sacrificing these mice, synaptic density was measured in hippocampus CA1 to assess the strength of hippocampal output. Mice submitted to RFS for 7 days showed decreased synaptic density in the hippocampus CA1, as demonstrated by reduced immunohistochemical staining for synaptophysin (Fig. 2a, left column; t-test, P<0.01, n=4 /group). Nuclear staining of HDAC2 was increased throughout the stratum pyramidale of CA1, consistent with previous literature showing that HDAC2 negatively regulates expression of SYP (41) (Fig. 2a, t-test, P<0.01, n=4/group). Finally, plasma corticosterone concentrations (measured in mid-afternoon) were significantly elevated in RFS-treated mice (Fig 1a. t-test, P=0.0047, n=4/group)

Again in experiments begun by a postdoctoral fellow and continued in collaboration, we tested the hypothesis that BLA cell body stimulation would be sufficient to replicate the cognitive and molecular effects of RFS. Three weeks after intra-BLA injection of AAV_5 virus encoding either

channelrhodopsin-2 (ChR2) or enhanced-yellow-fluorescent protein (eYFP) as a control (Fig. 1c), mice were begun on a seven-day paradigm of chronic BLA photostimulation using a 473 nm diode laser (See Fig. 1b for paradigm details; methods for complete description) after which the mice underwent cognitive testing, sacrifice, and tissue IHC analysis. ChR2/illuminated mice exhibited reduced synaptic density in CA1 (by SYP staining) (Fig 2b, t-test, *P*=0.0487, n=5/group), and increased intranuclear HDAC2 staining (Fig 2b, P=0.0018, n=5/group) compared to eYFP/illuminated controls. Comparison of ChR2-injected/illuminated experimental mice to eYFP-injected/illuminated control mice demonstrated cognitive and molecular effects similar to those of RFS: ChR2 treated mice showed no preference in the NOR task measured at 24 hours (Fig 2b, t-test *P*=0.0285, n= 10,12), and no preference in the NLR task measured at 1 hour (Fig. 2b, t-test, *P*=0.0416, n=12/group). eYFP animals showed normal preference in both cases. Plasma corticosterone concentration was elevated in eYFP/illuminated controls (relative to eYFP cage controls, data not shown, but see fig 2a for control), and there was significant further elevation in ChR2/illuminated animals (Fig 2b, t-test, *P*=0.0329, n=5/group)

Because these experiments suggested that the BLA is sufficient to replicate both hippocampus-dependent cognitive deficits as well as hippocampal molecular alterations normally associated with chronic stress, we wondered if BLA activation *during* stress was *necessary* for these same changes to occur. Experimental mice were injected AAV_5 encoding either eYFP, or the bioengineered inhibitory G-protein-coupled receptor hM4D(G_i) ("G_iDREADD"), which selectively inhibits CAMKII-expressing projection neurons of the BLA upon exposure to the exogenous ligand clozapine-N-oxide (CNO) (See methods and Fig 1. Panels D1-D3 for explanation and schematic). 30 minutes prior to

undergoing either the "context-only" control treatment, or RFS-treatment, all mice were injected with 0.3 mg/kg CNO IP. Given the pharmacokinetics of CNO as measured in humans and adjusting for the higher metabolic rate of the mouse by Kleiber's law, we calculated this dosage would result in a peak brain tissue concentration of approximately 12 mM, (Appendix Figure 1), which is above the 1mM-10mM concentrations shown to produce potent neuronal inhibition in slice preparations (121). Thusly we inhibited the BLA prior to stress treatment and repeated this procedure for 7 days, after which the mice underwent cognitive testing, sacrifice, and tissue IHC analysis as in previous experiments. Control animals (eYFP/CNO/"context only" and G_i-DREADD/CNO/"context-only") were behaviorally and molecularly identical to wild-type/"context only"-treated animals, and thus were grouped with controls from previous experiments (Figure 2C "eYFP/G_i + CNO CTRL"). G_iDREADD/CNO mediated inhibition of the BLA during RFS rescued synaptic density (Fig. 2c; ANOVA $P<0.0001$; Tukey post-hoc eYFP/CNO/RFS vs. GiDREADD/CNO/RFS, $P<0.0001$, n=4,5,6) and normalized HDAC2 expression (Fig 1c, one-Way ANOVA; Tukey's post-hoc, eYFP Con vs. eYFP RFS P<0.01, eYFP RFS vs Gi RFS P= n.s., n=4,5,6). Cognitive testing demonstrated that inhibiting the BLA during RFS (G_iDREADD/CNO/RFS treatment) also rescued hippocampus-dependent cognition, as demonstrated by restored performance in the NOR (t-test, $P=0.002$, n=16,15,7) and NLR (t-test, $P=0.0097$, n=10,10,7) tasks (Fig. 2c, right panels). The cognitive performance of G_iDREADD/CNO/RFS mice was not significantly different from control animals (Fig. 2c, one-Way ANOVA; Tukey's post-hoc, P= n.s., n=15, 16, 7).

Although these experiments suggest that glutamatergic cell activity in the BLA is somehow responsible for the effects of chronic stress, these neurons project broadly to many downstream targets. In order to determine if the direct BLA-to-hippocampus circuit was responsible for our observations, a postdoctoral fellow and I worked to photostimulate the ChR2-positive axon terminals of BLA afferent projections to the hippocampus. Having observed that BLA projection fibers arrived most densely to the *stratum oriens, lucidum* and *radiatum* of the CA3 field in our mice, we injected ChR2 into the BLA and implanted optical fibers 0.5 mm dorsal to CA3 in the dorsal hippocampus (bregma -2.18mm anteroposterior) (fig. 3a). Thereby we selectively modulated the activity of a direct BLA-to-hippocampus circuit.

The ChR2 or eYFP AAV_5 viral constructs were allowed 6 weeks for expression in order to increase channel density at the axon terminals (Fig. 3a). eYFP- and ChR2-injected mice were then begun on a seven-day photo-stimulation paradigm. In most cases, this paradigm was identical to that used for stimulation of the cell bodies (Fig. 1b); some animals received 20 sec bursts of constant illumination but after analysis were found to be molecularly and behaviorally identical to animals receiving 2 sec bursts (data not shown). ChR2-injected/terminal-illuminated mice again exhibited the same molecular changes as were observed in RFS-treated animals: reduced synaptic density in CA1 (by SYP staining) (Fig 3b, t-test, P=0.0069), and increased intranuclear HDAC2 staining (Fig 3b, t-test, P=0.0019). Photostimulation of BLA afferents in CA3 also produced a cognitive deficit in ChR2-injected/terminal-illumination animals, again demonstrated by lack of preference on the NOR (Fig. 3c, t-test, P=0.0057) and NLR (Figure 3c, t-test, P=0.0092) tasks compared to eYFP-injected/terminal-illumination treated controls. Plasma corticosterone concentration was not

elevated in ChR2-injected/terminal-illumination animals relative to eYFP-injected/terminal-illumination controls (Fig. 3d. ANOVA,P=0.087; Tukey post-hoc eYFP vs. ChR2, $P>0.05$), though both were elevated compared to eYFP-injected cage controls (Tukey post-hoc $P<0.05$, $P<0.05$). Also of note is that although overall concentrations did not differ between the experimental groups, they were high compared to previous experiments (Fig. 3d, Fig. 2a, Fig. 2b).

Having established that activation of a specific BLA circuit can replicate the effects of chronic-stress on the circuit target (in this case, the hippocampus), and given the myriad connections between chronic-stress and AD, I wondered if modulating BLA activity could alter the progression of hippocampal pathology in the 5xFAD murine model of AD.

I first sought to examine whether previous results that linked chronic stress and exacerbated AD pathology could be recapitulated in a mouse model of AD used in our lab. 5xFAD mice exhibited behavior suggesting they were resistant to stress in the RFS paradigm (Appendix Fig. 1c), and so I used 14 days of chronic restraint stress (CRS) to model chronic stress in 4 month-old 5xFAD animals (See Fig 1e and methods for complete description). CRS seemed to be an effective stressor in 5xFAD mice, as demonstrated by both increased plasma corticosterone concentration after a single CRS session (Fig.4a, t-test, $P=0.0013$, n=6,16), and decreased body mass after 14 days in CRS-treated animals compared to a net gain in controls (Fig. 4b, t-test, $P=0.0008$, n=6,10). CRS-treated animals had a higher number of 4G8-positive Aβ plaques throughout their hippocampus (Fig. 4c, t-test, $P=0.0115$ n=10,10). The Aβ-oligomer specific antibody Nu-1 was also used to assess Aβ oligomer density. This antibody is highly selective for Aβ oligomers (trimer, tetramer, 12-24mer)

and does not bind monomer peptides, thus would be expected to intensely label plaques and surrounding oligomer accumulations without background monomer binding (higher signal to noise in regards to plaque accumulation) (125). There was no significant increase in Aβ oligomer density in the DG, though a trend towards increased oligomers in CA1 was observed (Fig 4d, t-test, P=0.3575 CA1; P=0.1331 DG, n=3,6). There was no correlation between plasma corticosterone concentrations and hippocampal plaque load (Fig. 4e, r^2=0.0284, P=0.5181 n=17). Note that the graph in figure 4e includes data points from subsequent ChR2 BLA stimulation experiments. CRS-treated 5xFAD animals were not behaviorally tested, since the effects of various paradigms of acute and chronic stress in the 5xFAD model were difficult to characterize (see Appendix Fig. 1c, additional data not shown).

Next I tested whether photostimulation of the BLA in 5xFAD animals was sufficient to reproduce the phenotypic exacerbation that occurred with chronic stress. Using a modified paradigm (Fig. 1f) to adjust for possible stress resistance in the 5xFAD mice (Appendix Fig. 1c), photostimulation was applied to ChR2-injected or eYFP-injected control animals for 14 days. Plasma corticosterone was measured after a single illumination session and found to be elevated in the eYFP-injected/illuminated animals, but also significantly higher in ChR2-injected/illuminated animals (Fig. 5a; ANOVA P<0.0001; Tukey post-hoc eYFP vs. ChR2 P<0.05, n=5,10,10). After 14 days of BLA cell body photostimulation there was a trend towards increased hippocampal plaque load in ChR2-injected/illuminated mice compared to eYFP-injected/illuminated controls, measured by counting 4G8-positive Aβ plaques (Fig. 5b, t-test, P=0.217 n=4,5). There was also a significant increase in Aβ-oligomer density in the CA1 but not the DG (Fig. 1c, t-test, P=0.0448, n=9,12).

Despite this increase in Aβ staining, there was no increase in astrocyte activation/gliosis, as measured by the optical density of glial-fibrillary acidic protein (GFAP) in all strata of CA1 (Fig. 5d, t-test, *P*=0.835, n=5,5). Because 5xFAD mice show cognitive impairments in NOR and NOL tasks at 4 months (data not shown), I measured freezing levels as an approximation of contextual-fear-memory. ChR2-injected mice showed reduced contextual freezing levels after 14 days of BLA photostimulation, compared to eYFP-injected/illuminated controls (Fig. 5e. t-test, *P*=.0419, n=8,12). There was however no difference in cued freezing, suggesting normal amygdalohippocampal connectivity (Fig 5f, t-test, *P*=0.43, n=8,12)

Since BLA activation seemed to worsen AD pathology in 5xFAD mice, I wondered if chronically inactivating the BLA could slow progression of AD pathology, even absent any stressful experimental treatment. Three weeks after intra-BLA injection of AAV_5 virus encoding either GiDREADD or eYFP (using the same procedure as in previous experiments, Fig. d1-d3), I implanted subdermal osmotic pumps to deliver systemic CNO at a constant rate over 28 days (Fig. 6a). Using the same pharmacokinetic data as for previous calculations (See Appendix Fig. 1b) and the volume/flow rate parameters of our pumps, I calculated that osmotic pump delivery would sustain brain tissue CNO concentrations of 500nM over this 28 day experiment. Following this treatment, I observed a significant decrease in the density of Aβ oligomers in hippocampus CA1 of GiDREADD-injected/CNO-treated animals compared to eYFP-injected/CNO-treated controls (Fig 6b. t-test, *P*=0.0043, n=2,3). This same effect was not observed in the DG (Fig. 6b, t-test, *P*=0.63, n=2,3). (4G8 immunostaining was attempted but adequate experimental preparations were not achieved.) I again measured freezing levels as an approximation of hippocampal-cognition, and observed only a

slight trend towards increased freezing in GiDREADD-injected/CNO-treated animals compared to eYFP-injected/CNO-treated controls (Fig 6c, t-test, P=0.26, n=5,6). There was no trend suggested in cued freezing, suggesting normal amygdalohippocampal function (Fig. 6d. t-test, P=0.93, n=5,6). Because BLA inactivation was chronic in this paradigm, it was felt that measurement of plasma corticosterone would not be informative, and therefore this was not performed.

DISCUSSION

These results can be divided into two sections, each with their own implications. This first series of experiments (Figures 2, and 3) strongly suggest that activation of direct BLA projections can produce consistent molecular changes in the projection target (in this case the hippocampus), and also impair cognition that depends on that projection target. The second set (Figures 4, 5 and 6) suggests that modulating BLA activity in an AD model mouse may alter the progression of AD pathology in a BLA projection target, and also alter target-dependent cognition.

BLA Activity Underlies the Molecular and Cognitive Effects of Chronic Stress

Previous studies probing the effect of acute stress on cognitive function have found that inactivating the amygdala is sufficient to block both the behavioral and cellular effects of *acute* stress (126; 127). Specifically, electrolytic lesioning or pharmacological inactivation prevented alterations in hippocampal long term potentiation, and spatial memory deficits, both of which were induced by restraint or tailshock stress administered just prior to training (126; 127). Because our methods of activation and inactivation were highly specific, we can now assert that (1) excitatory activity of the BLA is both necessary and sufficient to produce the molecular effects of *chronic* stress on associated brain structures such as the hippocampus, and resultant cognitive effects, and (2) direct circuit connections are powerful and potentially causal contributions to the negative influences of psychological stress.

It is important to consider these results in the context of our corticosterone measurements, from which two related conclusions can be drawn. The first is that surgery and illumination increase plasma corticosterone concentrations significantly (Fig 2, Fig 5), but that photostimulation of the BLA results in even greater corticosterone release (Fig. 2, Fig. 5). The second is that terminal stimulation does not appear to elevate plasma corticosterone concentrations (Fig 3). Of note, the corticosterone concentrations of both eYFP and ChR2 injected mice were high in the terminal-illumination experiment. This might have been due to differences in surgical trauma (4 craniotomies instead of 2), handling, or sample collection.

Overall, these corticosterone results suggest that the changes in cognition, synaptic density, and HDAC2 staining we observed in terminal stimulation experiments occurred in the absence of increased peripheral corticosterone concentrations, which are known to act biphasically on the hippocampus and are often implicated in the effects of stress (70). They also suggest that in the terminal photostimulation experiments, antidromic propagation from the terminals to the cell body did not occur, or if so that the resultant depolarization was not sufficient to activate the soma of BLA neurons and drive further corticosterone release. We did not conduct experiments to silence the BLA pharmacologically while activating BLA terminals, and so we cannot claim that terminal stimulation did not result in antidromic propagation to the BLA. However, previous experiments using optogenetic stimulation of brain-slices revealed that antidromically driven activation of the somata occurred in only 5% of recordings, and in this experiment the terminals and cell bodies were separated by 300 μm, compared to many mm in our *in vivo* experiments (96).

However, our results do not absolve corticosterone and GR. Instead they demand an explanation that does not involve increased glucocorticoid concentration.

One possibility is that increased neuronal activity leads to phosphorylation of GR and altered downstream gene expression. Activity-dependent Ca^{2+} influx leads to increased activity of the tau-kinase protein Cdk5, through calpain-mediated cleavage of its activator protein p35 to the more stable p25 (128). Cdk5 can phosphorylate GR at multiple serine residues including S211, which alters recruitment of cofactors and can modify GR transcriptional activity (129). GR phosphorylation at S211 has also been found to increase nuclear recruitment, and modify transcriptional activation in a gene dependent manner (130). Thus without changes in corticosterone/cortisol concentration, driving neuronal activity through circuit activation could activate Cdk5, increasing GR phosphorylation and altering gene expression.

In our paradigm, ChR2 simulation of pyramidal neurons would induce significant elevation of hippocampal glutamate – previously observed using microdialysis following chronic stress (131). Imaging data from our experiments (not shown) suggested that in our mice, most BLA terminals arrive in the *stratum oriens, lucidum* and *radiatum* of the CA3 field. Hence BLA activity would lead to excitation of CA3, activation of Schaffer collaterals, and increased glutamate release in CA1. Coupled with even a relatively small excitatory drive from direct BLA afferents to CA1, this could lead to significant activation of the CA1 and potential allostatic or excitotoxic damage from excess glutamate release (132). Normally, this connectivity may allow the BLA-hippocampus axis to act in limbic-autoregulation by responding to both changes in corticosteroid concentration (through

hippocampal GR and MR binding), and to altered GR phosphorylation state via the activity of excitatory BLA afferents. However in states of chronic stress, increased glutamate release with altered transcriptional programming could lead to hippocampal maladaptation, and potentially even degeneration. Indeed the lifetime duration of major depression, (a disease known to involve amygdala hyperactivation and provide significant psychosocial stress) negatively correlates with hippocampal size (133).

Our results are the first to demonstrate that HDAC2 can be regulated by direct modulation of neural circuitry. As discussed above, this result may also be underlain by activity-dependent phosphorylation of GR, which our lab has previously shown to upregulate HDAC2 expression (40). Another recent study has suggested that HDAC2 regulation of glial-derived-neurotrophic-factor expression in the striatum is one determinant of the behavioral response to stress (134). Although our data do not allow us to claim that HDAC2 upregulation *causes* the molecular or cognitive deficits we observed, they do provide evidence for an epigenetic link between the pathophysiology of stress, and of AD.

BLA-driven Exacerbation of the AD Phenotype in 5xFAD Mice:

(i) Fear and Spatial Memory Abilities – Our results demonstrate that chronic BLA activation impairs spatial memory in 5xFAD mice, as measured by contextual freezing levels (Fig. 5). We also observed a maintenance of cued fear memory (Fig. 5, 6), which suggests that BLA function and amygdalohippocampal connectivity were preserved throughout these experiments (135). Taken together, these results suggest that enhanced BLA activity impairs hippocampus dependent cognition

in the 5xFAD murine model of AD. Our data also suggest that chronic inactivation has the potential to delay memory impairment in a preclinical AD model. A greater sample size is first needed to determine if these results (Fig. 6) are statistically significant.

It is important to note that our experiments cannot determine if impaired spatial memory in 5xFAD animals is due to the chronic-stress-like effect of BLA photostimulation (as in Figures 2 and 3), or truly accelerated AD-related cognitive decline. In future experiments, delaying cognitive testing of BLA-photostimulated 5xFAD mice for days to weeks would allow the effects of stress to wear off, while cognitive effects from accelerated disease progression would remain. Our chronic inhibition experiments demonstrate that even in the absence of chronic stress, modulating BLA activity can change AD pathology progression and the rate of cognitive decline. Taken together, these results would support the hypothesis that BLA activation alone is sufficient to accelerate AD-related cognitive decline.

(ii) Increased Aβ Plaque Pathology – Although overall Aβ plaque accumulation increased following chronic stress, consistent with previous literature, (figure 4), data from both activation and inactivation experiments suggested that Aβ load (both plaques and oligomers) could be altered most strongly in CA1, and was not changed in DG. (Note that analysis of CA1 was prioritized in the study of our 5xFAD mice – in contrast to the Swiss-Webster strain analyzed in figures 2 and 3 – since we did not directly examine the site of BLA afferents in the 5xFAD mouse, and classically the CA3 subfield receives fewer efferent BLA projections in the rodent and sends no reciprocal projections to the BLA in either rodent or primate (see introduction); further analysis would be

appropriate). The observations in CA1 are consistent with data from tracing studies in which CA1 is shown to receive excitatory projections from the BLA and also supply a strong reciprocal connection, while the DG neither receives nor returns excitatory BLA projections (106; 107; 109). Thus the distribution of Aβ plaque accumulation in our experiments suggests activity-dependent generation of Aβ – a hypothesis for which a wealth of literature offers support.

Much of the recent interest in activity-driven Aβ generation has stemmed from the discovery of the brain's "default network". Defined through fMRI to including prefrontal cortex, posterior cingulate cortex, inferior parietal lobule and hippocampal formation, the default network is active in introspective memory, self-reflection, and other forms of "internal cognition", and is perhaps the most active network across the human lifespan (136). Early in AD there is hypometabolism of these default network regions, and network dysfunction progresses more severely in AD than in normal aging (136). Moreover regional amyloid deposition and atrophy overlaps prominently with these default network regions (137).

In support of imaging data that links structural activation with Aβ accumulation, two lines of evidence can be drawn to a molecular underpinning between neuronal activity and Aβ production.

Firstly, rapid changes in Aβ production occur in response to modulating neuronal activity. *In vitro,* suppression of neuronal activity in brain slice preparations by either tetrodotoxin or high-Mg^{2+} can decrease APP processing and Aβ production, while neuronal activation by picrotoxin has the opposite effect (21). Immediate increases in Aβ production in response to neuronal activity can also

be observed *in vivo:* regional Aβ production correlates well with regional neuronal metabolism, and pharmacological modulation of neuronal activity can increase (with activation) or decrease (with inactivation) Aβ production and release into the interstitial fluid (ISF) as measured by *in vivo* microdialysis (138)(139). At a circuit level, experimental sensory deprivation can decrease Aβ plaque deposition specifically in the sensory cortex (138). Furthermore, the physiological activity modulation that occurs naturally during the sleep-wake cycle decreases Aβ production and release (140).

The cellular mechanism of activity-dependent Aβ production has also been elucidated. Neuronal activity and synaptic vesicle release lead to increase rates of membrane recycling through endocytosis at the presynaptic terminal. Transmembrane APP is thus internalized in endocytosed vescicles and cleaved by endosomal BACE-1, resulting in release of the Aβ fragment upon subsequent exocytosis (141)(142). Both basal and activity-regulated Aβ generation have been shown to depend on functional endocytosis (143), further suggesting that activity-driven changes are mediated through the synaptic release machinery.

As a second line of evidence, neuronal activity can also drive changes in expression of genes related to APP processing. The expression of BACE-1 and its enzymatic activity are both increased in response to oxidative stress, which might occur following intense neuronal activation. After oxidative stress, this increase in BACE-1 expression is mediated by phosphorylation of the immediate-early-gene product c-Jun by c-Jun N-terminal-kinase (JNK)(144; 145). There is also evidence that both JNK enzymatic activity and c-Jun phosphorylation increase after physiological neuronal activation,

following exposure to a novel environment (146), or after seizure induction by kainate administration (147). JNK mRNA expression is also regulated by sleep-wake cycle, suggesting that circadian rhythms can regulate the APP processing machinery (148) in addition to altering synaptic Aβ release. Another immediate early gene – *Arc* – is also involved in the trafficking of APP and association of APP with its processing machinery in the endosomes (149).

Thus neuronal activity can increase Aβ production in two ways: (1) through accelerated synaptic vesicle recycling, and (2) through genetic regulation of APP processing, via activation of immediate-early gene products.

The BLA and Acetylcholine

Key enzymes in the biosynthetic or catabolic pathways for acetylcholine are found in high density in the BLA. Choline-acetyltransferase (ChAT), acetylcholinesterase, and high-affinity choline transporters are often used as control markers to delineate the basolateral subnucleus of the BLA (78; 79), because the density of these markers is higher in the BLA than in any other forebrain structure (150). In normal aging, there is very little depletion of cholinergic innervations to the BLA, while in AD there is marked depletion of cholinergic markers in the neuropil, with high loss in the lateral nucleus, and relatively little loss in the basolateral nucleus (150). Thus the sensitivity of the cholinergic system to degeneration may feed forward to exacerbate BLA dysregulation in AD.

Therapeutic Potential

Studies of deep brain stimulation (DBS) in AD are ongoing. Pilot studies in 5 patients have demonstrated that stimulation of the hippocampal fornix can slow cognitive decline and normalize metabolic derangements in multiple neural networks throughout the brain (151; 152). The stimulators in these trials are inserted to lie parallel to the vertical portion of the hippocampal fornix, 2 mm dorsal to the optic tract at their ventral most extent, 5 mm from the midline. This would place these stimulators in the hypothalamus, and adjacent to the PVN – an important structure in regulation of the HPA axis. Although not mentioned by these authors, modulation of the limbic-stress axis might contribute to the effect of stimulation in these human patients.

Early intervention is crucial to a disease where the first symptoms arise decades after initial metabolic derangements occur. Should DBS prove therapeutically valuable in AD, there may be great promise in modulation of the stress axis. Suppressing the activity of the BLA through DBS may prove to have benefits in patients with MCI and a history of psychosocial distress, or longstanding neuropsychiatric disease.

Additional Experimental Limitations:

A major limitation of this study was leakage of AAV_5 virus into the central nucleus or along the injection tract. In all cases we analyzed amygdala expression of viral constructs to exclude mice with inaccurate injection, or excessive viral diffusion to surrounding regions. The vast majority of neurons in the centromedial amygdala (>95%) (including projection neurons) are GABAergic medium spiny neurons (153), which would not express our CaMKII-driven viral constructs. Additionally, cFos

data from immunohistochemical experiments demonstrated that there was no increase in activation of the central nucleus beyond that of eYFP controls, even when viral expression extended into the central nuclei (data not shown). This may have been due to fiber optic placement, or feed-forward inhibition from the centrolateral nucleus to the centromedial nucleus upon BLA activation (96).

Fear conditioning testing was used in 5xFAD mice because deficits were identified in more low-stress tasks (NOR, NLR) in 4-month old untreated mice. Nevertheless, fear conditioning is a stressful cognitive test in an experiment designed to examine the effects of chronic stress. Because fear-memory is potentiated by stress, we expected increased freezing in BLA photostimulated mice. Since cued freezing was unchanged and contextual freezing was in fact reduced in experimentally treated 5xFAD mice, we believe these measures accurately reflect cognitive abilities.

Our study used exclusively male 5xFAD mice. There are many known differences between sexes in both central (especially limbic), peripheral, and behavioral effects of chronic stress (154) . Although this study focused on specific activation of direct circuit projections and sought to exclude the influence of the peripheral stress axis, it is possible there are also differences in central circuits and structural connectivity in male and female mice (and by extension primates) that affect the generalizability of this study.

Finally, our experiments assume that 500 nM concentration of CNO is sufficient to suppress neuronal activity. Although significant results in the opposite direction as BLA activation suggest

effective chronic BLA suppression did occur, this concentration is somewhat lower than used in previous literature (121)(123), and so should be tested in slice preparation.

CONCLUSIONS:

In brief, we believe that these results suggest that activation of BLA circuits can lead to molecular dysfunction in directly connected regions, and impair target-dependent cognition. Activity-dependent perturbations in neuronal function, and alterations in glucocorticoid signaling may underlie these effects. Our results also characterize HDAC2 as an epigenetic link between chronic stress and AD, and suggest that processes involved in maladaptation to chronic stress in an otherwise healthy brain may also accelerate progression of disease in the AD brain. Finally, our experiments suggest that modulating BLA activity can alter the progression of pathology and cognitive decline in a mouse model of AD.

SUMMARY

(1) In Swiss-Webster mice, chronic stress (RFS, 7 days) acts to decrease synaptic density in the hippocampus and increase expression of HDAC2. Hippocampus-dependent cognition is also impaired, as measured by novel-object and novel-location discrimination abilities.

(2) Activity of glutamatergic projections neurons in the basolateral nuclear group of the amygdala (BLA) is both necessary and sufficient to produce the molecular and cognitive effects of chronic stress on the hippocampus. Furthermore, activation of direct BLA projections within the hippocampus also leads to decreased synaptic density, increased HDAC2 expression, and impaired hippocampus-dependent cognition, implicating the direct BLA-to-hippocampus circuit in the effects of chronic stress.

(3) Chronic-restraint-stress is an effective model of chronic stress in 5xFAD mice. Like in other mouse models of AD, stress worsens AD-like neuropathology in 5xFAD mice.

(4) Chronic ChR2-mediated BLA photostimulation (14 days) is sufficient to increase AD-like neuropathology in 5xFAD mice, and impair cognition.

(5) Chronic G_iDREADD-mediated BLA inactivation (28 days) slows the development of AD-like neuropathology in 5xFAD mice, and may improve cognition relative to untreated 5xFAD controls.

REFERENCES

1. Association A. Alzheimer's disease facts and figures. Alzheimer's Dement. 2014;10(2)
2. Hebert LE, Weuve J, Scherr P, Evans D. Alzheimer disease in the United States (2010-2050) estimated using the 2010 census. [Internet]. Neurology 2013 Feb;[cited 2013 Mar 5] Available from: http://www.ncbi.nlm.nih.gov/pubmed/23390181
3. American Psychiatric Association. Diagnostic and Statistical Manual of Mental Disorders, Fifth Edition. 5th ed. Washington, DC: Author; 2013.
4. Devanand D, Jacobs D, Tang M-X, Del Castillo-Castaneda C, Sano M, Marder K, Bell K, Bylsma F, Brandt J, Albers M, Stern Y. The course of psychopathologic features in mild to moderate Alzheimer's disease. Arch. Gen. Psychiatry 1997;54(3):257 –263.
5. Jack CR, Albert MS, Knopman DS, McKhann GM, Sperling R a, Carrillo MC, Thies B, Phelps CH. Introduction to the recommendations from the National Institute on Aging-Alzheimer's Association workgroups on diagnostic guidelines for Alzheimer's disease. [Internet]. Alzheimers. Dement. 2011 May;7(3):257–62.[cited 2013 Mar 2] Available from: http://www.pubmedcentral.nih.gov/articlerender.fcgi?artid=3096735&tool=pmcentrez&rendertype=abstract
6. Braak H, Braak E. Acta H ' pathologica Neuropathological stageing of Alzheimer-related changes. 1991;239–259.
7. Hardy JA, Higgins GA. The Amyloid Cascade Hypothesis. Science (80-.). 1992;256(5054):184–185.
8. Davies P, Maloney AJF. Selective Loss of Central Cholinergic Neurons in Alzheimer's Disease. Lancet 1976;2(8000):1403.
9. Francis PT, Palmer M, Snape M, Wilcock GK. The cholinergic hypothesis of Alzheimer's disease: a review of progress [Internet]. J. Neurol. Neurosurg. Psychiatry 1999 Feb;66(2):137–147.Available from: http://jnnp.bmj.com/cgi/doi/10.1136/jnnp.66.2.137
10. Knapp MJ, Knopman DS, Solomon PR, William W, Davis CS, Gracon SI. A 30-Week Randomized Controlled Trial of High-Dose Tacrine in Patients With Alzheimer ' s Disease. J. Am. Med. Assoc. 1994;271(13):985–991.
11. Rösler M, Anand R, Cicin-sain A, Gauthier S, Agid Y, Dal-bianco P. Efficacy and safety of rivastigmine in patients with Alzheimer ' s disease: international randomised controlled trial. Br. Med. J. 1999;518:633–640.
12. Raschetti R, Albanese E, Vanacore N, Maggini M. Cholinesterase inhibitors in mild cognitive impairment: a systematic review of randomised trials. [Internet]. PLoS Med. 2007 Nov;4(11):e338.[cited 2013 Apr 15] Available from: http://www.pubmedcentral.nih.gov/articlerender.fcgi?artid=2082649&tool=pmcentrez&rendertype=abstract
13. O'Brien RJ, Wong PC. Amyloid precursor protein processing and Alzheimer's disease. [Internet]. Annu. Rev. Neurosci. 2011 Jan;34:185–204.[cited 2013 Mar 5] Available from: http://www.pubmedcentral.nih.gov/articlerender.fcgi?artid=3174086&tool=pmcentrez&rendertype=abstract

14. Haass C, Selkoe DJ. Soluble protein oligomers in neurodegeneration: lessons from the Alzheimer's amyloid beta-peptide. [Internet]. Nat. Rev. Mol. Cell Biol. 2007 Feb;8(2):101–12.[cited 2013 Feb 28] Available from: http://www.ncbi.nlm.nih.gov/pubmed/17245412
15. Haass C. Take five--BACE and the gamma-secretase quartet conduct Alzheimer's amyloid beta-peptide generation. [Internet]. EMBO J. 2004 Feb;23(3):483–8.[cited 2013 Feb 27] Available from: http://www.pubmedcentral.nih.gov/articlerender.fcgi?artid=1271800&tool=pmcentrez&rendertype=abstract
16. Luo Y, Bolon B, Kahn S, Bennett BD, Babu-khan S, Denis P, Fan W, Kha H, Zhang J, Gong Y, Martin L, Louis J, Yan Q, Richards WG, Citron M, Vassar R. Mice deficient in BACE1 , the Alzheimer ' s gamma-secretase , have normal phenotype and abolished β-amyloid generation. 2001;3–4.
17. Senechal Y, Kelly PH, Dev KK. Amyloid precursor protein knockout mice show age-dependent deficits in passive avoidance learning. [Internet]. Behav. Brain Res. 2008 Jan;186(1):126–32.[cited 2013 Apr 16] Available from: http://www.ncbi.nlm.nih.gov/pubmed/17884188
18. Young-Pearse TL, Bai J, Chang R, Zheng JB, LoTurco JJ, Selkoe DJ. A critical function for beta-amyloid precursor protein in neuronal migration revealed by in utero RNA interference. [Internet]. J. Neurosci. 2007 Dec;27(52):14459–69.[cited 2013 Mar 10] Available from: http://www.ncbi.nlm.nih.gov/pubmed/18160654
19. Nikolaev A, McLaughlin T, O'Leary DDM, Tessier-Lavigne M. APP binds DR6 to trigger axon pruning and neuron death via distinct caspases. [Internet]. Nature 2009 Feb;457(7232):981–9.[cited 2013 Mar 5] Available from: http://www.pubmedcentral.nih.gov/articlerender.fcgi?artid=2677572&tool=pmcentrez&rendertype=abstract
20. Nalivaeva NN, Turner AJ. The amyloid precursor protein: A biochemical enigma in brain development, function and disease [Internet]. FEBS Lett. 2013;587(13):2046–2054.Available from: http://dx.doi.org/10.1016/j.febslet.2013.05.010
21. Kamenetz F, Tomita T, Hsieh H, Seabrook G, Borchelt D, Iwatsubo T, Sisodia S, Malinow R. APP Processing and Synaptic Function. 2003;37:925–937.
22. Yankner B a, Dawes LR, Fisher S, Villa-Komaroff L, Oster-Granite ML, Neve RL. Neurotoxicity of a fragment of the amyloid precursor associated with Alzheimer's disease. [Internet]. Science 1989 Jul;245(4916):417–20.Available from: http://www.ncbi.nlm.nih.gov/pubmed/2474201
23. Jin M, Shepardson N, Yang T, Chen G, Walsh D, Selkoe DJ. Soluble amyloid beta-protein dimers isolated from Alzheimer cortex directly induce Tau hyperphosphorylation and neuritic degeneration. [Internet]. Proc. Natl. Acad. Sci. U. S. A. 2011 Apr;108(14):5819–24.[cited 2013 Mar 1] Available from: http://www.pubmedcentral.nih.gov/articlerender.fcgi?artid=3078381&tool=pmcentrez&rendertype=abstract
24. De Felice FG, Wu D, Lambert MP, Fernandez SJ, Velasco PT, Lacor PN, Bigio EH, Jerecic J, Acton PJ, Shughrue PJ, Chen-Dodson E, Kinney GG, Klein WL. Alzheimer's disease-type neuronal tau hyperphosphorylation induced by A beta oligomers. [Internet]. Neurobiol.

Aging 2008 Sep;29(9):1334–47.[cited 2012 Nov 13] Available from: http://www.pubmedcentral.nih.gov/articlerender.fcgi?artid=3142933&tool=pmcentrez&rendertype=abstract
25. Lee MS, Kwon YT, Li M, Peng J, Friedlander RM, Tsai LH. Neurotoxicity induces cleavage of p35 to p25 by calpain. [Internet]. Nature 2000 May;405(6784):360–4.Available from: http://www.ncbi.nlm.nih.gov/pubmed/10830966
26. Um J, Kaufman A, Kostylev M, Heiss J, Stagi M, Takahashi H, Kerrisk M, Vortmeyer A, Wisniewski T, Koleske A, Gunther E, Nygaard H, Strittmatter S. Metabotropic Glutamate Receptor 5 Is a Coreceptor for Alzheimer A Oligomer Bound to Cellular Prion Protein [Internet]. Neuron 2013;79(5):887–902.Available from: http://dx.doi.org/10.1016/j.neuron.2013.06.036
27. Rushworth J V., Griffiths HH, Watt NT, Hooper NM. Prion protein-mediated toxicity of amyloid-beta oligomers requires lipid rafts and the transmembrane LRP1. J. Biol. Chem. 2013;288(13):8935–8951.
28. Shankar GM, Li S, Mehta TH, Garcia-Munoz A, Shepardson NE, Smith I, Brett FM, Farrell M a, Rowan MJ, Lemere C a, Regan CM, Walsh DM, Sabatini BL, Selkoe DJ. Amyloid-beta protein dimers isolated directly from Alzheimer's brains impair synaptic plasticity and memory. [Internet]. Nat. Med. 2008 Aug;14(8):837–42.[cited 2013 Feb 27] Available from: http://www.pubmedcentral.nih.gov/articlerender.fcgi?artid=2772133&tool=pmcentrez&rendertype=abstract
29. Bertram L, Lill CM, Tanzi RE. The genetics of Alzheimer disease: back to the future. [Internet]. Neuron 2010 Oct;68(2):270–81.[cited 2013 Feb 27] Available from: http://www.ncbi.nlm.nih.gov/pubmed/20955934
30. Rumble B, Retallack R, Hilbich C, Simms G, Multhaup G, Martins R, Hockey A, Montgomery P, Beyreuther K, Masters C. Amyloid A4 Protein and its Precursor in Down's Syndrome and Alzheimer's Disease. N. Engl. J. Med. 1989;320(22):1446–1452.
31. Jonsson T, Atwal JK, Steinberg S, Snaedal J, Jonsson P V, Bjornsson S, Stefansson H, Sulem P, Gudbjartsson D, Maloney J, Hoyte K, Gustafson A, Liu Y, Lu Y, Bhangale T, Graham RR, Huttenlocher J, Bjornsdottir G, Andreassen O a, Jönsson EG, Palotie A, Behrens TW, Magnusson OT, Kong A, Thorsteinsdottir U, Watts RJ, Stefansson K. A mutation in APP protects against Alzheimer's disease and age-related cognitive decline. [Internet]. Nature 2012 Aug;488(7409):96–9.[cited 2013 Feb 27] Available from: http://www.ncbi.nlm.nih.gov/pubmed/22801501
32. Jonsson T, Stefansson H, Ph.D. SS, Jonsdottir I, Jonsson P V., Snaedal J, Bjornsson S, Huttenlocher J, Levey AI, Lah JJ, Rujescu D, Hampel H, Giegling I, Andreassen O a., Engedal K, Ulstein I, Djurovic S, Ibrahim-Verbaas C, Hofman A, Ikram MA, van Duijn CM, Thorsteinsdottir U, Kong A, Stefansson K. Variant of TREM2 Associated with the Risk of Alzheimer's Disease [Internet]. N. Engl. J. Med. 2012 Nov;121114152813005.[cited 2012 Nov 15] Available from: http://www.nejm.org/doi/abs/10.1056/NEJMoa1211103
33. Guerreiro R, Wojtas A, Bras J, Carrasquillo M, Rogaeva E, Majounie E, Cruchaga C, Sassi C, Kauwe JSK, Younkin S, Hazrati L, Collinge J, Pocock J, Lashley T, Williams J, Lambert J-C, Amouyel P, Goate A, Rademakers R, Morgan K, Powell J, St. George-Hyslop P, Singleton A, Hardy J. TREM2 Variants in Alzheimer's Disease [Internet]. N. Engl. J. Med. 2012

Nov;121114171407007.[cited 2012 Nov 15] Available from: http://www.nejm.org/doi/abs/10.1056/NEJMoa1211851

34. Cruchaga C, Karch CM, Jin SC, Benitez B a, Cai Y, Guerreiro R, Harari O, Norton J, Budde J, Bertelsen S, Jeng AT, Cooper B, Skorupa T, Carrell D, Levitch D, Hsu S, Choi J, Ryten M, Hardy J, Trabzuni D, Weale ME, Ramasamy A, Smith C, Sassi C, Bras J, Gibbs JR, Hernandez DG, Lupton MK, Powell J, Forabosco P, Ridge PG, Corcoran CD, Tschanz JT, Norton MC, Munger RG, Schmutz C, Leary M, Demirci FY, Bamne MN, Wang X, Lopez OL, Ganguli M, Medway C, Turton J, Lord J, Braae A, Barber I, Brown K, Passmore P, Craig D, Johnston J, McGuinness B, Todd S, Heun R, Kölsch H, Kehoe PG, Hooper NM, Vardy ERLC, Mann DM, Pickering-Brown S, Kalsheker N, Lowe J, Morgan K, David Smith a, Wilcock G, Warden D, Holmes C, Pastor P, Lorenzo-Betancor O, Brkanac Z, Scott E, Topol E, Rogaeva E, Singleton AB, Kamboh MI, St George-Hyslop P, Cairns N, Morris JC, Kauwe JSK, Goate AM. Rare coding variants in the phospholipase D3 gene confer risk for Alzheimer's disease. [Internet]. Nature 2014;505(7484):550–4.Available from: http://www.ncbi.nlm.nih.gov/pubmed/24336208
35. Melchior B, Garcia AE, Hsiung B-K, Lo KM, Doose JM, Thrash JC, Stalder AK, Staufenbiel M, Neumann H, Carson MJ. Dual induction of TREM2 and tolerance-related transcript, Tmem176b, in amyloid transgenic mice: implications for vaccine-based therapies for Alzheimer's disease. [Internet]. ASN Neuro 2010 Jan;2(3):e00037.[cited 2013 Apr 1] Available from: http://www.pubmedcentral.nih.gov/articlerender.fcgi?artid=2905103&tool=pmcentrez&rendertype=abstract
36. Oakley H, Cole SL, Logan S, Maus E, Shao P, Craft J, Guillozet-Bongaarts A, Ohno M, Disterhoft J, Van Eldik L, Berry R, Vassar R. Intraneuronal beta-amyloid aggregates, neurodegeneration, and neuron loss in transgenic mice with five familial Alzheimer's disease mutations: potential factors in amyloid plaque formation. [Internet]. J. Neurosci. 2006 Oct;26(40):10129–40.[cited 2013 Mar 1] Available from: http://www.ncbi.nlm.nih.gov/pubmed/17021169
37. Davis DG, Schmitt FA, Wekstein DR, Markesbery WR. Alzheimer Neuropathologic Alterations in Aged Cognitively Normal Subjects. 1999;376–388.
38. Savva GM, Wharton SB, Ince PG, Forster G, Matthews FE, Brayne C. Age, Neuropathology, and Dementia. 2009;
39. Bateman RJ, Xiong C, Benzinger TLS, Fagan AM, Goate A, Fox NC, Marcus DS, Cairns NJ, Xie X, Blazey TM, Holtzman DM, Santacruz A, Buckles V, Oliver A, Moulder K, Aisen PS, Ghetti B, Klunk WE, McDade E, Martins RN, Masters CL, Mayeux R, Ringman JM, Rossor MN, Schofield PR, Sperling R a, Salloway S, Morris JC. Clinical and biomarker changes in dominantly inherited Alzheimer's disease. [Internet]. N. Engl. J. Med. 2012 Aug;367(9):795–804.[cited 2013 Feb 27] Available from: http://www.ncbi.nlm.nih.gov/pubmed/22784036
40. Gräff J, Rei D, Guan J-S, Wang W-Y, Seo J, Hennig KM, Nieland TJF, Fass DM, Kao PF, Kahn M, Su SC, Samiei A, Joseph N, Haggarty SJ, Delalle I, Tsai L-H. An epigenetic blockade of cognitive functions in the neurodegenerating brain. [Internet]. Nature 2012 Mar;483(7388):222–6.[cited 2013 Feb 27] Available from:

http://www.pubmedcentral.nih.gov/articlerender.fcgi?artid=3498952&tool=pmcentrez&rendertype=abstract
41. Guan J-S, Haggarty SJ, Giacometti E, Dannenberg J-H, Joseph N, Gao J, Nieland TJF, Zhou Y, Wang X, Mazitschek R, Bradner JE, DePinho R a, Jaenisch R, Tsai L-H. HDAC2 negatively regulates memory formation and synaptic plasticity. [Internet]. Nature 2009 May;459(7243):55–60.[cited 2013 Feb 27] Available from: http://www.pubmedcentral.nih.gov/articlerender.fcgi?artid=3498958&tool=pmcentrez&rendertype=abstract
42. Geda YE, Roberts RO, Knopman DS, Petersen RC, Christianson TJH, Pankratz VS, Smith GE, Boeve BF. Prevalence of Neuropsychiatric Symptoms in Mild Cognitive Impairment and Normal Cognitive Aging. Arch. Gen. Psychiatry 2008;65(10):1193–1198.
43. Lyketsos CG, Steinberg M, Tschanz JT, Norton MC, Steffens DC, Breitner JC. Mental and behavioral disturbances in dementia: findings from the Cache County Study on Memory in Aging. [Internet]. Am. J. Psychiatry 2000 May;157(5):708–14.Available from: http://www.ncbi.nlm.nih.gov/pubmed/10784462
44. Steinberg M, Sheppard J, Tschanz JT, Ph D, Norton MC, Steffens DC, Breitner JCS, Lyketsos CG. and Behavioral Disturbances in Dementia: The Cache County Study. J. Neuropsychiatry Clin. Neurosci. 2003;15(3):340–345.
45. Costa PT, McCrae RR. NEO Five-Factor Inventory (NEO-FFI). 2003;
46. Wilson RS, Barnes LL, Bennett D a, Li Y, Bienias JL, Mendes de Leon CF, Evans D a. Proneness to psychological distress and risk of Alzheimer disease in a biracial community. [Internet]. Neurology 2005 Jan;64(2):380–2.Available from: http://www.ncbi.nlm.nih.gov/pubmed/15668449
47. Wilson RS, Schneider J, Boyle P, Arnold SE, Tang Y, Bennett D a. Chronic distress and incidence of mild cognitive impairment. [Internet]. Neurology 2007 Jun;68(24):2085–92.[cited 2013 Apr 18] Available from: http://www.ncbi.nlm.nih.gov/pubmed/17562829
48. Fischer P, Jungwirth S, Zehetmayer S, Weissgram S, Hoenigschnabl S, Gelpi E, Krampla W, Tragl KH. Conversion from subtypes of mild cognitive impairment to Alzheimer dementia. [Internet]. Neurology 2007 Jan;68(4):288–91.[cited 2012 Sep 16] Available from: http://www.ncbi.nlm.nih.gov/pubmed/17242334
49. Monastero R, Mangialasche F, Camarda C, Ercolani S, Camarda R. A systematic review of neuropsychiatric symptoms in mild cognitive impairment. [Internet]. J. Alzheimers. Dis. 2009 Jan;18(1):11–30.[cited 2012 Sep 16] Available from: http://www.ncbi.nlm.nih.gov/pubmed/19542627
50. Chan WC, Lam LCW, Tam CWC, Lui VWC, Leung GTY, Lee ATC, Chan SSM, Fung AWT, Chiu HFK, Chan WM. Neuropsychiatric symptoms are associated with increased risks of progression to dementia: a 2-year prospective study of 321 Chinese older persons with mild cognitive impairment. [Internet]. Age Ageing 2011 Jan;40(1):30–5.[cited 2013 Mar 19] Available from: http://www.ncbi.nlm.nih.gov/pubmed/21106558
51. Palmer K, Berger a K, Monastero R, Winblad B, Bäckman L, Fratiglioni L. Predictors of progression from mild cognitive impairment to Alzheimer disease. [Internet]. Neurology 2007 May;68(19):1596–602.[cited 2013 Apr 21] Available from: http://www.ncbi.nlm.nih.gov/pubmed/17485646

52. Teng E, Lu PH, Cummings JL. Neuropsychiatric symptoms are associated with progression from mild cognitive impairment to Alzheimer's disease. [Internet]. Dement. Geriatr. Cogn. Disord. 2007 Jan;24(4):253–9.[cited 2013 Mar 17] Available from: http://www.ncbi.nlm.nih.gov/pubmed/17700021
53. Richard E, Reitz C, Honig LH, Schupf N, Tang MX, Manly JJ, Mayeux R, Devanand D, Luchsinger J a. Late-Life Depression, Mild Cognitive Impairment, and Dementia. [Internet]. Arch. Neurol. 2012 Dec;70(3):1–7.[cited 2013 Mar 6] Available from: http://www.ncbi.nlm.nih.gov/pubmed/23277390
54. Rapp M a, Schnaider-Beeri M, Grossman HT, Sano M, Perl DP, Purohit DP, Gorman JM, Haroutunian V. Increased hippocampal plaques and tangles in patients with Alzheimer disease with a lifetime history of major depression. [Internet]. Arch. Gen. Psychiatry 2006 Feb;63(2):161–7.Available from: http://www.ncbi.nlm.nih.gov/pubmed/16461859
55. Ownby RL, Crocco E, Acevedo A, John V, Loewenstein D. Depression and the risk of Alzheimer disease [Internet]. Arch. Gen. Psychiatry 2006;63:530–538.[cited 2012 Sep 16] Available from: http://journals.lww.com/epidem/Abstract/2005/03000/Depression_and_the_Risk_of_Alzheimer_Disease.13.aspx
56. Carroll B, Feinberg M, Greden J, Tarika J, Albala A, Haskett R, James N, Kronfol Z, Lohr N, Steiner M, de Vigne J, Young E. A specific laboratory test for the diagnosis of melancholia. Standardization, validation, and clinical utility. Achives Gen. Psychiatry [date unknown];38(1):15–22.
57. Greenwald B, Mathé A, Mohs R, Levy M, Johns C, Davis K. Cortisol and Alzheimer's disease, II: Dexamethasone suppression, dementia severity, and affective symptoms. Am. J. Psychiatry 1986;143(4):442–6.
58. Wahbeh H, Kishiyama SS, Zajdel D, Oken BS. Salivary Cortisol Awakening Response in Mild Alzheimer. 2008;22(2):181–183.
59. Kudoh a, Ishihara H, Matsuki a. Response to surgical stress in elderly patients and Alzheimer's disease. [Internet]. Can. J. Anaesth. 1999 Mar;46(3):247–52.Available from: http://www.ncbi.nlm.nih.gov/pubmed/10210049
60. Csernansky JG, Dong H, Fagan AM, Wang L, Xiong C, Holtzman DM, Morris JC. Plasma cortisol and progression of dementia in subjects with Alzheimer-type dementia. [Internet]. Am. J. Psychiatry 2006 Dec;163(12):2164–9.Available from: http://www.pubmedcentral.nih.gov/articlerender.fcgi?artid=1780275&tool=pmcentrez&rendertype=abstract
61. Aisen PS, Davis KL, Berg JD, Schafer K, Campbell K, Thomas RG, Weiner MF, Farlow MR, Sano M, Grundman M, Thal LJ. A randomized controlled trial of prednisone in Alzheimer's disease [Internet]. Neurology 2000 Feb;54(3):588–588.[cited 2013 Apr 21] Available from: http://www.neurology.org/cgi/doi/10.1212/WNL.54.3.588
62. Raadsheer F, van Heerikhuize J, Lucassen P, Hoogendijk W, Tilders F, Swaab D. Corticotropin-Releasing Hormone mRNA Levels in the Paraventricular Nucleus of Patients With Alzheimer's Disease and Depression. Am. J. Psychiatry 1995;152:1372–1376.
63. Dong H, Goico B, Martin M, Csernansky C a, Bertchume a, Csernansky JG. Modulation of hippocampal cell proliferation, memory, and amyloid plaque deposition in APPsw (Tg2576)

mutant mice by isolation stress. [Internet]. Neuroscience 2004 Jan;127(3):601–9.[cited 2013 Mar 28] Available from: http://www.ncbi.nlm.nih.gov/pubmed/15283960
64. Hsiao Y-H, Chen PS, Chen S-H, Gean P-W. The involvement of Cdk5 activator p35 in social isolation-triggered onset of early Alzheimer's disease-related cognitive deficit in the transgenic mice. [Internet]. Neuropsychopharmacology 2011 Aug;36(9):1848–58.[cited 2012 Sep 16] Available from: http://www.pubmedcentral.nih.gov/articlerender.fcgi?artid=3154103&tool=pmcentrez&rendertype=abstract
65. Rothman SM, Herdener N, Camandola S, Texel SJ, Mughal MR, Cong W-N, Martin B, Mattson MP. 3xTgAD mice exhibit altered behavior and elevated Aβ after chronic mild social stress. [Internet]. Neurobiol. Aging 2012 Apr;33(4):830.e1–12.[cited 2012 Sep 3] Available from: http://www.ncbi.nlm.nih.gov/pubmed/21855175
66. Green KN, Billings LM, Roozendaal B, McGaugh JL, LaFerla FM. Glucocorticoids increase amyloid-beta and tau pathology in a mouse model of Alzheimer's disease. [Internet]. J. Neurosci. 2006 Aug;26(35):9047–56.[cited 2013 Jan 30] Available from: http://www.ncbi.nlm.nih.gov/pubmed/16943563
67. Cole M a, Kim PJ, Kalman B a, Spencer RL. Dexamethasone suppression of corticosteroid secretion: evaluation of the site of action by receptor measures and functional studies. [Internet]. Psychoneuroendocrinology 2000 Feb;25(2):151–67.Available from: http://www.ncbi.nlm.nih.gov/pubmed/10674279
68. Kang J-E, Cirrito JR, Dong H, Csernansky JG, Holtzman DM. Acute stress increases interstitial fluid amyloid-beta via corticotropin-releasing factor and neuronal activity. [Internet]. Proc. Natl. Acad. Sci. U. S. A. 2007 Jun;104(25):10673–8.Available from: http://www.pubmedcentral.nih.gov/articlerender.fcgi?artid=1965571&tool=pmcentrez&rendertype=abstract
69. Dong H, Murphy KM, Meng L, Montalvo-Ortiz J, Zeng Z, Kolber BJ, Zhang S, Muglia LJ, Csernansky JG. Corticotrophin releasing factor accelerates neuropathology and cognitive decline in a mouse model of Alzheimer's disease. [Internet]. J. Alzheimers. Dis. 2012 Jan;28(3):579–92.[cited 2013 May 16] Available from: http://www.pubmedcentral.nih.gov/articlerender.fcgi?artid=3494090&tool=pmcentrez&rendertype=abstract
70. De Kloet ER, Joëls M, Holsboer F. Stress and the brain: from adaptation to disease. [Internet]. Nat. Rev. Neurosci. 2005 Jun;6(6):463–75.[cited 2013 Mar 3] Available from: http://www.ncbi.nlm.nih.gov/pubmed/15891777
71. Nolte J. The Human Brain: An Introduction to its Functional Neuroanatomy. 6th ed. Philadelphia: Mosby Elselvier; 2006.
72. Anderson P, Morris R, Amaral D, Bliss T, O'Keefe J. The Hippocampus Book. New York: Oxford University Press; 2007.
73. Scoviille WB, Milner B. LOSS OF RECENT MEMORY AFTER BILATERAL HIPPOCAMPAL LESIONS. J. Neurol. Neurosurg. Psychiatry 1957;20:11–21.
74. Bliss T, Lomo T. Long lasting potentiation of synaptic transmission in the dentate area of the anaesthetized rabbit following stimulation of the perforant path. J. Physiol. 1973;232:331–356.

75. Vargha-Khadem F, Gadian DG, Watkins KE, Connelly a, Van Paesschen W, Mishkin M. Differential effects of early hippocampal pathology on episodic and semantic memory. [Internet]. Science 1997 Jul;277(5324):376–80.Available from: http://www.ncbi.nlm.nih.gov/pubmed/9219696
76. Eldridge LL, Knowlton BJ, Furmanski CS, Bookheimer SY, Engel S a. Remembering episodes: a selective role for the hippocampus during retrieval. [Internet]. Nat. Neurosci. 2000 Nov;3(11):1149–52.Available from: http://www.ncbi.nlm.nih.gov/pubmed/11036273
77. O'Keefe J, Dostrovsky J. The hippocampus as a spatial map. Preliminary evidence from unit activity in the freely-moving rat. Brain Res. 1971;34(1):171–175.
78. Yilmazer-Hanke DM. Amygdala. In: Paxinos G, Mai J, editors. The Human Nervous System. Elselvier; 2012
79. Heimer L, De Olmos J, Alheid G, Pearson J, Sakamoto N, Shinoda K, Marsteiner J, Switcer R. The Human Basal Forebrain, Part II. Part 3. In: Bloom F, Bjorklund A, Hokfelt T, editors. Handbook of Chemical Neuroanatomy: The Primate Nervous System, Volume 15. Elselvier; 1999 p. 57–226.
80. Solano-Castiella E, Anwander A, Lohmann G, Weiss M, Docherty C, Geyer S, Reimer E, Friederici AD, Turner R. Diffusion tensor imaging segments the human amygdala in vivo. [Internet]. Neuroimage 2010 Feb;49(4):2958–65.[cited 2013 Feb 28] Available from: http://www.ncbi.nlm.nih.gov/pubmed/19931398
81. Bzdok D, Laird AR, Zilles K, Fox PT, Eickhoff SB. An investigation of the structural, connectional, and functional subspecialization in the human amygdala. [Internet]. Hum. Brain Mapp. 2012 Jul;000(November 2011)[cited 2013 Mar 5] Available from: http://www.ncbi.nlm.nih.gov/pubmed/22806915
82. Herman JP, Cullinan WE. Neurocircuitry of stress: central control of the hypothalamo-pituitary-adrenocortical axis. [Internet]. Trends Neurosci. 1997 Mar;20(2):78–84.Available from: http://www.ncbi.nlm.nih.gov/pubmed/9023876
83. Baram TZ, Hatalski CG. Neuropeptide-mediated excitability: a key triggering mechanism for seizure generation in the developing brain. [Internet]. Trends Neurosci. 1998 Nov;21(11):471–6.Available from: http://www.pubmedcentral.nih.gov/articlerender.fcgi?artid=3372323&tool=pmcentrez&rendertype=abstract
84. Chen Y, Brunson KL, Müller MB, Cariaga W, Baram TZ. Immunocytochemical distribution of corticotropin-releasing hormone receptor type-1 (CRF(1))-like immunoreactivity in the mouse brain: light microscopy analysis using an antibody directed against the C-terminus. [Internet]. J. Comp. Neurol. 2000 May;420(3):305–23.Available from: http://www.pubmedcentral.nih.gov/articlerender.fcgi?artid=3119344&tool=pmcentrez&rendertype=abstract
85. Herman JP. Stress Response : Neural and Feedback Regulation of the HPA Axis. 2009;505–510.
86. Morales-Medina JC, Sanchez F, Flores G, Dumont Y, Quirion R. Morphological reorganization after repeated corticosterone administration in the hippocampus, nucleus accumbens and amygdala in the rat. [Internet]. J. Chem. Neuroanat. 2009 Dec;38(4):266–72.[cited 2013 Apr 2] Available from: http://www.ncbi.nlm.nih.gov/pubmed/19505571

87. Erdmann G, Berger S, Schütz G. Genetic dissection of glucocorticoid receptor function in the mouse brain. [Internet]. J. Neuroendocrinol. 2008 Jun;20(6):655–9.[cited 2013 May 21] Available from: http://www.ncbi.nlm.nih.gov/pubmed/18513206
88. Ledoux JE. Emotion Circuits in the Brain. Annu. Rev. Neurosci. 2000;23:155–184.
89. Shin LM, Liberzon I. The neurocircuitry of fear, stress, and anxiety disorders. [Internet]. Neuropsychopharmacology 2010 Jan;35(1):169–91.[cited 2013 Mar 1] Available from: http://www.pubmedcentral.nih.gov/articlerender.fcgi?artid=3055419&tool=pmcentrez&rendertype=abstract
90. Sananes CB, Davis M. N-methyl-D-aspartate lesions of the lateral and basolateral nuclei of the amygdala block fear-potentiated startle and shock sensitization of startle. [Internet]. Behav. Neurosci. 1992 Feb;106(1):72–80.Available from: http://www.ncbi.nlm.nih.gov/pubmed/1554439
91. Cheng DT, Knight DC, Smith CN, Helmstetter FJ. Human amygdala activity during the expression of fear responses. [Internet]. Behav. Neurosci. 2006 Dec;120(6):1187–95.[cited 2013 Mar 11] Available from: http://www.ncbi.nlm.nih.gov/pubmed/17201461
92. Bishop SJ, Duncan J, Lawrence AD. State anxiety modulation of the amygdala response to unattended threat-related stimuli. [Internet]. J. Neurosci. 2004 Nov;24(46):10364–8.[cited 2013 Mar 4] Available from: http://www.ncbi.nlm.nih.gov/pubmed/15548650
93. Cahill L, Haier RJ, Fallon J, Alkire MT, Tang C, Keator D, Wu J, McGaugh JL. Amygdala activity at encoding correlated with long-term, free recall of emotional information. [Internet]. Proc. Natl. Acad. Sci. U. S. A. 1996 Jul;93(15):8016–21.Available from: http://www.pubmedcentral.nih.gov/articlerender.fcgi?artid=38867&tool=pmcentrez&rendertype=abstract
94. Fanselow M, Gale G. The Amygdala, Fear, and Memory. Ann. N. Y. Acad. Sci. 2003;985:125–134.
95. Alvarez RP, Biggs A, Chen G, Pine DS, Grillon C. Contextual fear conditioning in humans: cortical-hippocampal and amygdala contributions. [Internet]. J. Neurosci. 2008 Jun;28(24):6211–9.[cited 2013 Mar 20] Available from: http://www.pubmedcentral.nih.gov/articlerender.fcgi?artid=2475649&tool=pmcentrez&rendertype=abstract
96. Tye KM, Prakash R, Kim S-Y, Fenno LE, Grosenick L, Zarabi H, Thompson KR, Gradinaru V, Ramakrishnan C, Deisseroth K. Amygdala circuitry mediating reversible and bidirectional control of anxiety. [Internet]. Nature 2011 Mar;471(7338):358–62.[cited 2012 Jul 17] Available from: http://www.pubmedcentral.nih.gov/articlerender.fcgi?artid=3154022&tool=pmcentrez&rendertype=abstract
97. LeDoux JE, Iwata J, Cicchetti P, Reis DJ. Different projections of the central amygdaloid nucleus mediate autonomic and behavioral correlates of conditioned fear. [Internet]. J. Neurosci. 1988 Jul;8(7):2517–29.Available from: http://www.ncbi.nlm.nih.gov/pubmed/2854842
98. Kim S-Y, Adhikari A, Lee SY, Marshel JH, Kim CK, Mallory CS, Lo M, Pak S, Mattis J, Lim BK, Malenka RC, Warden MR, Neve R, Tye KM, Deisseroth K. Diverging neural pathways assemble a behavioural state from separable features in anxiety. [Internet]. Nature 2013

Apr;496(7444):219–23.[cited 2013 May 21] Available from: http://www.ncbi.nlm.nih.gov/pubmed/23515158
99. Ehrlich I, Humeau Y, Grenier F, Ciocchi S, Herry C, Lüthi A. Amygdala inhibitory circuits and the control of fear memory. [Internet]. Neuron 2009 Jun;62(6):757–71.[cited 2013 May 21] Available from: http://www.ncbi.nlm.nih.gov/pubmed/19555645
100. McGaugh JL. The amygdala modulates the consolidation of memories of emotionally arousing experiences. [Internet]. Annu. Rev. Neurosci. 2004 Jan;27:1–28.[cited 2012 Jul 16] Available from: http://www.ncbi.nlm.nih.gov/pubmed/15217324
101. Roozendaal B, McEwen BS, Chattarji S. Stress, memory and the amygdala. [Internet]. Nat. Rev. Neurosci. 2009 Jun;10(6):423–33.[cited 2012 Jul 24] Available from: http://www.ncbi.nlm.nih.gov/pubmed/19469026
102. McIntyre CK, Miyashita T, Setlow B, Marjon KD, Steward O, Guzowski JF, McGaugh JL. Memory-influencing intra-basolateral amygdala drug infusions modulate expression of Arc protein in the hippocampus. [Internet]. Proc. Natl. Acad. Sci. U. S. A. 2005 Jul;102(30):10718–23.[cited 2013 May 4] Available from: http://www.pubmedcentral.nih.gov/articlerender.fcgi?artid=1175582&tool=pmcentrez&rendertype=abstract
103. Luine V, Villegas M, Martinez C, McEwen BS. Repeated stress causes reversible impairments of spatial memory performance. [Internet]. Brain Res. 1994 Mar;639(1):167–70.Available from: http://www.ncbi.nlm.nih.gov/pubmed/8180832
104. Vyas A, Mitra R, Shankaranarayana Rao BS, Chattarji S. Chronic stress induces contrasting patterns of dendritic remodeling in hippocampal and amygdaloid neurons. [Internet]. J. Neurosci. 2002 Aug;22(15):6810–8.Available from: http://www.ncbi.nlm.nih.gov/pubmed/12151561
105. Padival M, Quinette D, Rosenkranz JA. Effects of repeated stress on excitatory drive of basal amygdala neurons in vivo. [Internet]. Neuropsychopharmacology 2013;38(9):1748–62.Available from: http://www.ncbi.nlm.nih.gov/pubmed/23535779
106. Aggleton JP. A description of the amygdalo-hippocampal interconnections in the macaque monkey. Exp. Brain Res. 1986;64:515–526.
107. Saunders RC, Rosene DL, Van Hoesen GW. Comparison of the efferents of the amygdala and the hippocampal formation in the rhesus monkey: II. Reciprocal and non-reciprocal connections. [Internet]. J. Comp. Neurol. 1988 May;271(2):185–207.Available from: http://www.ncbi.nlm.nih.gov/pubmed/2454247
108. Pitkänen a, Pikkarainen M, Nurminen N, Ylinen a. Reciprocal connections between the amygdala and the hippocampal formation, perirhinal cortex, and postrhinal cortex in rat. A review. [Internet]. Ann. N. Y. Acad. Sci. 2000 Jun;911:369–91.Available from: http://www.ncbi.nlm.nih.gov/pubmed/10911886
109. Pikkarainen M, Rönkkö S, Savander V, Insausti R, Pitkänen a. Projections from the lateral, basal, and accessory basal nuclei of the amygdala to the hippocampal formation in rat. [Internet]. J. Comp. Neurol. 1999 Jan;403(2):229–60.Available from: http://www.ncbi.nlm.nih.gov/pubmed/9886046
110. Sheline YI, Barch DM, Donnelly JM, Ollinger JM, Snyder a Z, Mintun M a. Increased amygdala response to masked emotional faces in depressed subjects resolves with

antidepressant treatment: an fMRI study. [Internet]. Biol. Psychiatry 2001 Nov;50(9):651–8.Available from: http://www.ncbi.nlm.nih.gov/pubmed/11704071
111. Rauch SL, Whalen PJ, Shin LM, McInerney SC, Macklin ML, Lasko NB, Orr SP, Pitman RK. Exaggerated amygdala response to masked facial stimuli in posttraumatic stress disorder: a functional MRI study. [Internet]. Biol. Psychiatry 2000 May;47(9):769–76.Available from: http://www.ncbi.nlm.nih.gov/pubmed/10812035
112. Harmer CJ, Mackay CE, Reid CB, Cowen PJ, Goodwin GM. Antidepressant drug treatment modifies the neural processing of nonconscious threat cues. [Internet]. Biol. Psychiatry 2006 May;59(9):816–20.[cited 2013 Mar 10] Available from: http://www.ncbi.nlm.nih.gov/pubmed/16460693
113. Benson BE, Willis MW, Ketter T a., Speer A, Kimbrell T a., Herscovitch P, George MS, Post RM. Differential abnormalities of functional connectivity of the amygdala and hippocampus in unipolar and bipolar affective disorders [Internet]. J. Affect. Disord. 2014;168:243–253.Available from: http://dx.doi.org/10.1016/j.jad.2014.05.045
114. Yao H, Liu Y, Zhou B, Zhang Z, An N, Wang P, Wang L, Zhang X, Jiang T. Decreased functional connectivity of the amygdala in Alzheimer's disease revealed by resting-state fMRI [Internet]. Eur. J. Radiol. 2013;82(9):1531–1538.Available from: http://dx.doi.org/10.1016/j.ejrad.2013.03.019
115. Mistridis P, Taylor KI, Kissler JM, Monsch AU, Kressig RW, Kivisaari SL. Distinct neural systems underlying reduced emotional enhancement for positive and negative stimuli in early Alzheimer's disease. [Internet]. Front. Hum. Neurosci. 2013;7(January):939.Available from: http://www.pubmedcentral.nih.gov/articlerender.fcgi?artid=3895803&tool=pmcentrez&rendertype=abstract
116. Mori E, Ikeda M, Nobutsugu H, Kitagaki H, Imamura T, Shimomura T. Amygdalar Volume and Emotional Memory in Alzheimer ' s Disease. Am. J. Psychiatry 1999;156(2):216–222.
117. Poulin SP, Dautoff R, Morris JC, Barrett LF, Dickerson BC. Amygdala atrophy is prominent in early Alzheimer's disease and relates to symptom severity. [Internet]. Psychiatry Res. 2011 Oct;194(1):7–13.[cited 2013 Apr 1] Available from: http://www.pubmedcentral.nih.gov/articlerender.fcgi?artid=3185127&tool=pmcentrez&rendertype=abstract
118. Horínek D, Petrovický P, Hort J, Krásenský J, Brabec J, Bojar M, Vanecková M, Seidl Z. Amygdalar volume and psychiatric symptoms in Alzheimer's disease: an MRI analysis. [Internet]. Acta Neurol. Scand. 2006 Jan;113(1):40–5.[cited 2013 Apr 1] Available from: http://www.ncbi.nlm.nih.gov/pubmed/16367898
119. Zhang F, Gradinaru V, Adamantidis AR, Durand R, Airan RD, de Lecea L, Deisseroth K. Optogenetic interrogation of neural circuits: technology for probing mammalian brain structures. [Internet]. Nat. Protoc. 2010 Mar;5(3):439–56.[cited 2012 Jul 17] Available from: http://www.ncbi.nlm.nih.gov/pubmed/20203662
120. Cardin J a, Carlén M, Meletis K, Knoblich U, Zhang F, Deisseroth K, Tsai L-H, Moore CI. Targeted optogenetic stimulation and recording of neurons in vivo using cell-type-specific expression of Channelrhodopsin-2. [Internet]. Nat. Protoc. 2010 Feb;5(2):247–54.[cited 2012 Jul 16] Available from: http://www.ncbi.nlm.nih.gov/pubmed/20134425

121. Armbruster BN, Li X, Pausch MH, Herlitze S, Roth BL. Evolving the lock to fit the key to create a family of G protein-coupled receptors potently activated by an inert ligand. [Internet]. Proc. Natl. Acad. Sci. U. S. A. 2007 Mar;104(12):5163–8.Available from: http://www.pubmedcentral.nih.gov/articlerender.fcgi?artid=1829280&tool=pmcentrez&rendertype=abstract
122. Dong S, Rogan SC, Roth BL. Directed molecular evolution of DREADDs: a generic approach to creating next-generation RASSLs. [Internet]. Nat. Protoc. 2010 Mar;5(3):561–73.[cited 2012 Oct 9] Available from: http://www.ncbi.nlm.nih.gov/pubmed/20203671
123. Krashes MJ, Koda S, Ye C, Rogan SC, Adams AC, Cusher DS, Maratos-flier E, Roth BL, Lowell BB. Brief report Rapid , reversible activation of AgRP neurons drives feeding behavior in mice. 2011;121(4):2–6.
124. Paxinos G, Franklin K. The mouse brain in stereotaxis coordinates. San Diego: Elselvier Science; 2001.
125. Lambert MP, Velasco PT, Chang L, Viola KL, Fernandez S, Lacor PN, Khuon D, Gong Y, Bigio EH, Shaw P, De Felice FG, Krafft G a, Klein WL. Monoclonal antibodies that target pathological assemblies of Abeta. [Internet]. J. Neurochem. 2007 Jan;100(1):23–35.[cited 2012 Nov 12] Available from: http://www.ncbi.nlm.nih.gov/pubmed/17116235
126. Kim JJ, Koo JW, Lee HJ, Han J-S. Amygdalar inactivation blocks stress-induced impairments in hippocampal long-term potentiation and spatial memory. [Internet]. J. Neurosci. 2005 Feb;25(6):1532–9.[cited 2012 Nov 9] Available from: http://www.ncbi.nlm.nih.gov/pubmed/15703407
127. Kim JJ, Lee HJ, Han JS, Packard MG. Amygdala is critical for stress-induced modulation of hippocampal long-term potentiation and learning. [Internet]. J. Neurosci. 2001 Jul;21(14):5222–8.Available from: http://www.ncbi.nlm.nih.gov/pubmed/11438597
128. Su SC, Tsai L-H. Cyclin-dependent kinases in brain development and disease. [Internet]. Annu. Rev. Cell Dev. Biol. 2011 Jan;27:465–91.[cited 2013 Apr 12] Available from: http://www.ncbi.nlm.nih.gov/pubmed/21740229
129. Kino T, Ichijo T, Amin ND, Kesavapany S, Wang Y, Kim N, Rao S, Player A, Zheng Y-L, Garabedian MJ, Kawasaki E, Pant HC, Chrousos GP. Cyclin-dependent kinase 5 differentially regulates the transcriptional activity of the glucocorticoid receptor through phosphorylation: clinical implications for the nervous system response to glucocorticoids and stress. [Internet]. Mol. Endocrinol. 2007 Jul;21(7):1552–68.[cited 2013 Apr 10] Available from: http://www.ncbi.nlm.nih.gov/pubmed/17440046
130. Chen W, Dang T, Blind RD, Wang Z, Cavasotto CN, Hittelman AB, Rogatsky I, Logan SK, Garabedian MJ. Glucocorticoid receptor phosphorylation differentially affects target gene expression. [Internet]. Mol. Endocrinol. 2008 Aug;22(8):1754–66.[cited 2012 Nov 5] Available from: http://www.pubmedcentral.nih.gov/articlerender.fcgi?artid=2725771&tool=pmcentrez&rendertype=abstract
131. Moghaddam B. Stress preferentially increases extraneuronal levels of excitatory amino acids in the prefrontal cortex: comparison to hippocampus and basal ganglia. [Internet]. J. Neurochem. 1993 May;60(5):1650–7.Available from: http://www.ncbi.nlm.nih.gov/pubmed/8097232

132. McEwan B, Stellar E. Stress and the Individual. Arch. Intern. Med. 1993;153:2093–2101.
133. Sheline YI, Sanghavi M, Mintun M a, Gado MH. Depression duration but not age predicts hippocampal volume loss in medically healthy women with recurrent major depression. [Internet]. J. Neurosci. 1999 Jun;19(12):5034–43.Available from: http://www.ncbi.nlm.nih.gov/pubmed/10366636
134. Uchida S, Hara K, Kobayashi A, Otsuki K, Yamagata H, Hobara T, Suzuki T, Miyata N, Watanabe Y. Epigenetic status of Gdnf in the ventral striatum determines susceptibility and adaptation to daily stressful events. [Internet]. Neuron 2011 Jan;69(2):359–72.[cited 2013 Mar 16] Available from: http://www.ncbi.nlm.nih.gov/pubmed/21262472
135. Phillips RG, LeDoux JE. Differential contribution of amygdala and hippocampus to cued and contextual fear conditioning. [Internet]. Behav. Neurosci. 1992 Apr;106(2):274–85.Available from: http://www.ncbi.nlm.nih.gov/pubmed/1590953
136. Buckner RL, Andrews-Hanna JR, Schacter DL. The brain's default network: anatomy, function, and relevance to disease. [Internet]. Ann. N. Y. Acad. Sci. 2008 Mar;1124:1–38.[cited 2012 Jul 12] Available from: http://www.ncbi.nlm.nih.gov/pubmed/18400922
137. Buckner RL, Snyder AZ, Shannon BJ, LaRossa G, Sachs R, Fotenos AF, Sheline YI, Klunk WE, Mathis C a, Morris JC, Mintun M a. Molecular, structural, and functional characterization of Alzheimer's disease: evidence for a relationship between default activity, amyloid, and memory. [Internet]. J. Neurosci. 2005 Aug;25(34):7709–17.[cited 2013 Mar 1] Available from: http://www.ncbi.nlm.nih.gov/pubmed/16120771
138. Bero AW, Yan P, Roh JH, Cirrito JR, Stewart FR, Raichle ME, Lee J-M, Holtzman DM. Neuronal activity regulates the regional vulnerability to amyloid-β deposition. [Internet]. Nat. Neurosci. 2011 Jun;14(6):750–6.[cited 2013 Feb 27] Available from: http://www.pubmedcentral.nih.gov/articlerender.fcgi?artid=3102784&tool=pmcentrez&rendertype=abstract
139. Cirrito JR, Yamada K a, Finn MB, Sloviter RS, Bales KR, May PC, Schoepp DD, Paul SM, Mennerick S, Holtzman DM. Synaptic activity regulates interstitial fluid amyloid-beta levels in vivo. [Internet]. Neuron 2005 Dec;48(6):913–22.[cited 2013 Feb 27] Available from: http://www.ncbi.nlm.nih.gov/pubmed/16364896
140. Kang J-E, Lim MM, Bateman RJ, Lee JJ, Smyth LP, Cirrito JR, Fujiki N, Nishino S, Holtzman DM. Amyloid-beta dynamics are regulated by orexin and the sleep-wake cycle. [Internet]. Science 2009 Nov;326(5955):1005–7.[cited 2013 Mar 7] Available from: http://www.pubmedcentral.nih.gov/articlerender.fcgi?artid=2789838&tool=pmcentrez&rendertype=abstract
141. O'Brien RJ, Wong PC. Amyloid precursor protein processing and Alzheimer's disease. [Internet]. Annu. Rev. Neurosci. 2011 Jan;34:185–204.[cited 2012 Jul 13] Available from: http://www.pubmedcentral.nih.gov/articlerender.fcgi?artid=3174086&tool=pmcentrez&rendertype=abstract
142. Vassar R. Beta-Secretase Cleavage of Alzheimer's Amyloid Precursor Protein by the Transmembrane Aspartic Protease BACE [Internet]. Science (80-.). 1999 Oct;286(5440):735–741.[cited 2013 Mar 16] Available from: http://www.sciencemag.org/cgi/doi/10.1126/science.286.5440.735

143. Cirrito JR, Kang J-E, Lee J, Stewart FR, Verges DK, Silverio LM, Bu G, Mennerick S, Holtzman DM. Endocytosis is required for synaptic activity-dependent release of amyloid-beta in vivo. [Internet]. Neuron 2008 Apr;58(1):42–51.[cited 2013 Feb 27] Available from: http://www.pubmedcentral.nih.gov/articlerender.fcgi?artid=2390913&tool=pmcentrez&rendertype=abstract
144. Tamagno E, Guglielmotto M, Aragno M, Borghi R, Autelli R, Giliberto L, Muraca G, Danni O, Zhu X, Smith M a, Perry G, Jo D-G, Mattson MP, Tabaton M. Oxidative stress activates a positive feedback between the gamma- and beta-secretase cleavages of the beta-amyloid precursor protein. [Internet]. J. Neurochem. 2008 Feb;104(3):683–95.[cited 2013 Feb 28] Available from: http://www.pubmedcentral.nih.gov/articlerender.fcgi?artid=2220052&tool=pmcentrez&rendertype=abstract
145. Tamagno E, Parola M, Bardini P, Piccini A, Borghi R, Guglielmotto M, Santoro G, Davit A, Danni O, Smith M a, Perry G, Tabaton M. Beta-site APP cleaving enzyme up-regulation induced by 4-hydroxynonenal is mediated by stress-activated protein kinases pathways. [Internet]. J. Neurochem. 2005 Feb;92(3):628–36.[cited 2013 Mar 16] Available from: http://www.ncbi.nlm.nih.gov/pubmed/15659232
146. Xu X, Raber J, Yang D, Su B, Mucke L. Dynamic regulation of c-Jun N-terminal kinase activity in mouse brain by environmental stimuli. [Internet]. Proc. Natl. Acad. Sci. U. S. A. 1997 Nov;94(23):12655–60.Available from: http://www.pubmedcentral.nih.gov/articlerender.fcgi?artid=25073&tool=pmcentrez&rendertype=abstract
147. Mielke K, Brecht S, Dorst a, Herdegen T. Activity and expression of JNK1, p38 and ERK kinases, c-Jun N-terminal phosphorylation, and c-jun promoter binding in the adult rat brain following kainate-induced seizures. [Internet]. Neuroscience 1999 Jan;91(2):471–83.Available from: http://www.ncbi.nlm.nih.gov/pubmed/10366004
148. Cirelli C, Tononi G. Gene expression in the brain across the sleep-waking cycle. [Internet]. Brain Res. 2000 Dec;885(2):303–21.Available from: http://www.ncbi.nlm.nih.gov/pubmed/11102586
149. Wu J, Petralia RS, Kurushima H, Patel H, Jung M, Volk L, Chowdhury S, Shepherd JD, Dehoff M, Li Y, Kuhl D, Huganir RL, Price DL, Scannevin R, Troncoso JC, Wong PC, Worley PF. Arc/Arg3.1 regulates an endosomal pathway essential for activity-dependent β-amyloid generation. [Internet]. Cell 2011 Oct;147(3):615–28.[cited 2012 Jul 30] Available from: http://www.ncbi.nlm.nih.gov/pubmed/22036569
150. Emre M, Heckers S, Mash DC, Geula C, Mesulam MM. Cholinergic innervation of the amygdaloid complex in the human brain and its alterations in old age and Alzheimer's disease. [Internet]. J. Comp. Neurol. 1993 Oct;336(1):117–34.Available from: http://www.ncbi.nlm.nih.gov/pubmed/8254109
151. Smith GS, Laxton AW, Tang-Wai DF, McAndrews MP, Diaconescu AO, Workman CI, Lozano AM. Increased cerebral metabolism after 1 year of deep brain stimulation in Alzheimer disease. [Internet]. Arch. Neurol. 2012 Sep;69(9):1141–8.[cited 2012 Nov 8] Available from: http://www.ncbi.nlm.nih.gov/pubmed/22566505

152. Laxton AW, Tang-Wai DF, McAndrews MP, Zumsteg D, Wennberg R, Keren R, Wherrett J, Naglie G, Hamani C, Smith GS, Lozano AM. A phase I trial of deep brain stimulation of memory circuits in Alzheimer's disease. [Internet]. Ann. Neurol. 2010 Oct;68(4):521–34.[cited 2012 Nov 7] Available from: http://www.ncbi.nlm.nih.gov/pubmed/20687206
153. McDonald A. Cytoarchitecture of the central amygdaloid nucleus of the rat. J. Comp. Neurol. 1982;208(4):401–18.
154. Mclaughlin K, Baran SE, Conrad CE. Chronic Stress- and Sex-Specific Neuromorphological and Functional Changes in Limbic Structures. Mol. Neurobiol. 2009;40(2):166–82.

Figure 1

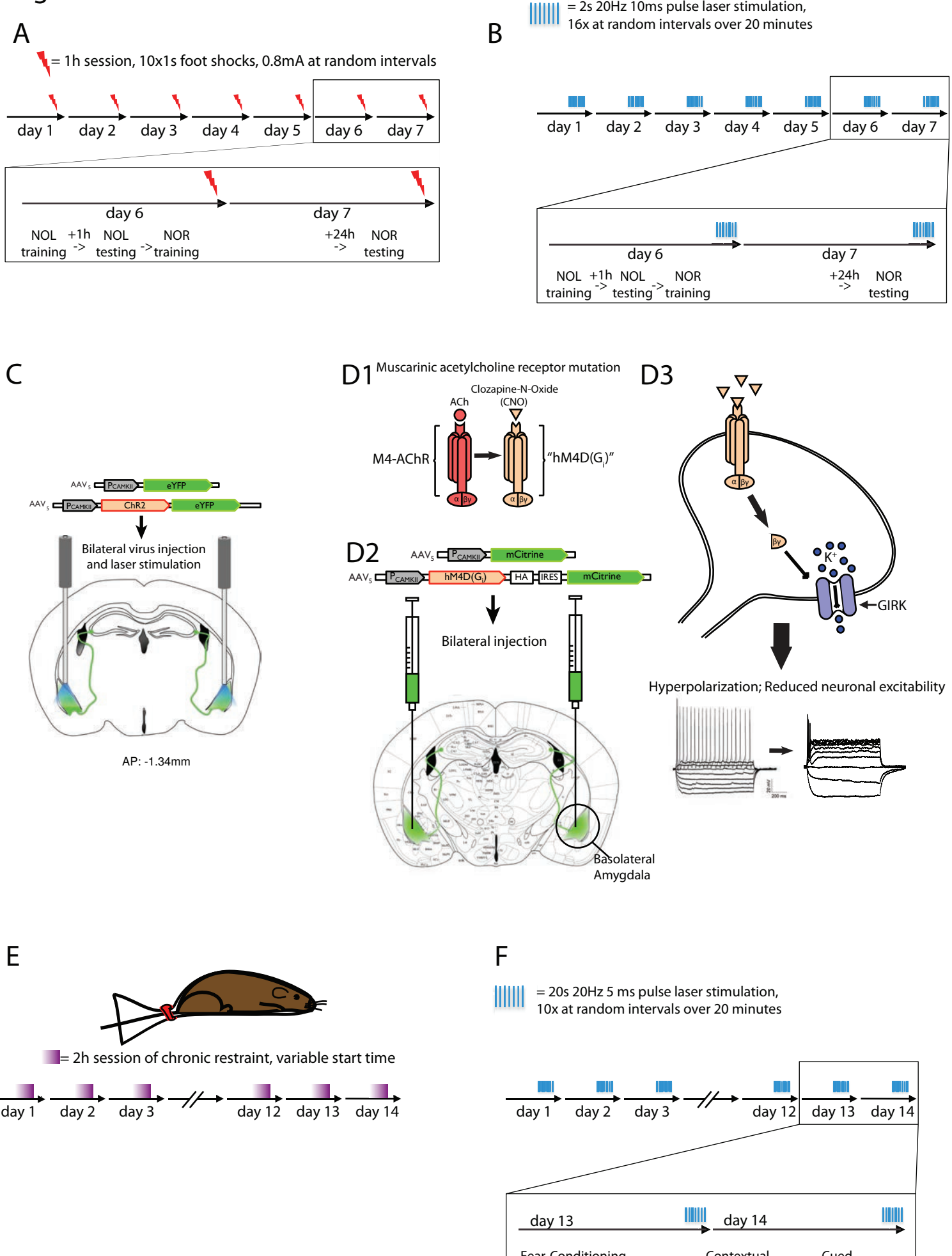
A
= 1h session, 10x1s foot shocks, 0.8mA at random intervals
day 1
day 2
day 3
day 4
day 5
day 6
day 7
day 6
day 7
NOL training
+1h ->
NOL testing
-> NOR training
+24h ->
NOR testing
B
= 2s 20Hz 10ms pulse laser stimulation, 16x at random intervals over 20 minutes
day 1
day 2
day 3
day 4
day 5
day 6
day 7
day 6
day 7
NOL training
+1h ->
NOL testing
-> NOR training
+24h ->
NOR testing
C
AAV5 PCAMKII eYFP
AAV5 PCAMKII ChR2 eYFP
Bilateral virus injection and laser stimulation
AP: -1.34mm
D1
Muscarinic acetylcholine receptor mutation
Clozapine-N-Oxide (CNO)
ACh
M4-AChR
"hM4D(Gi)"
D2
AAV5 PCAMKII mCitrine
AAV5 PCAMKII hM4D(Gi) HA IRES mCitrine
Bilateral injection
Basolateral Amygdala
D3
GIRK
Hyperpolarization; Reduced neuronal excitability
E
= 2h session of chronic restraint, variable start time
day 1
day 2
day 3
day 12
day 13
day 14
F
= 20s 20Hz 5 ms pulse laser stimulation, 10x at random intervals over 20 minutes
day 1
day 2
day 3
day 12
day 13
day 14
day 13
day 14
Fear-Conditioning Training
+24h ->
Contextual Testing
+ 6h ->
Cued Testing

Figure 2

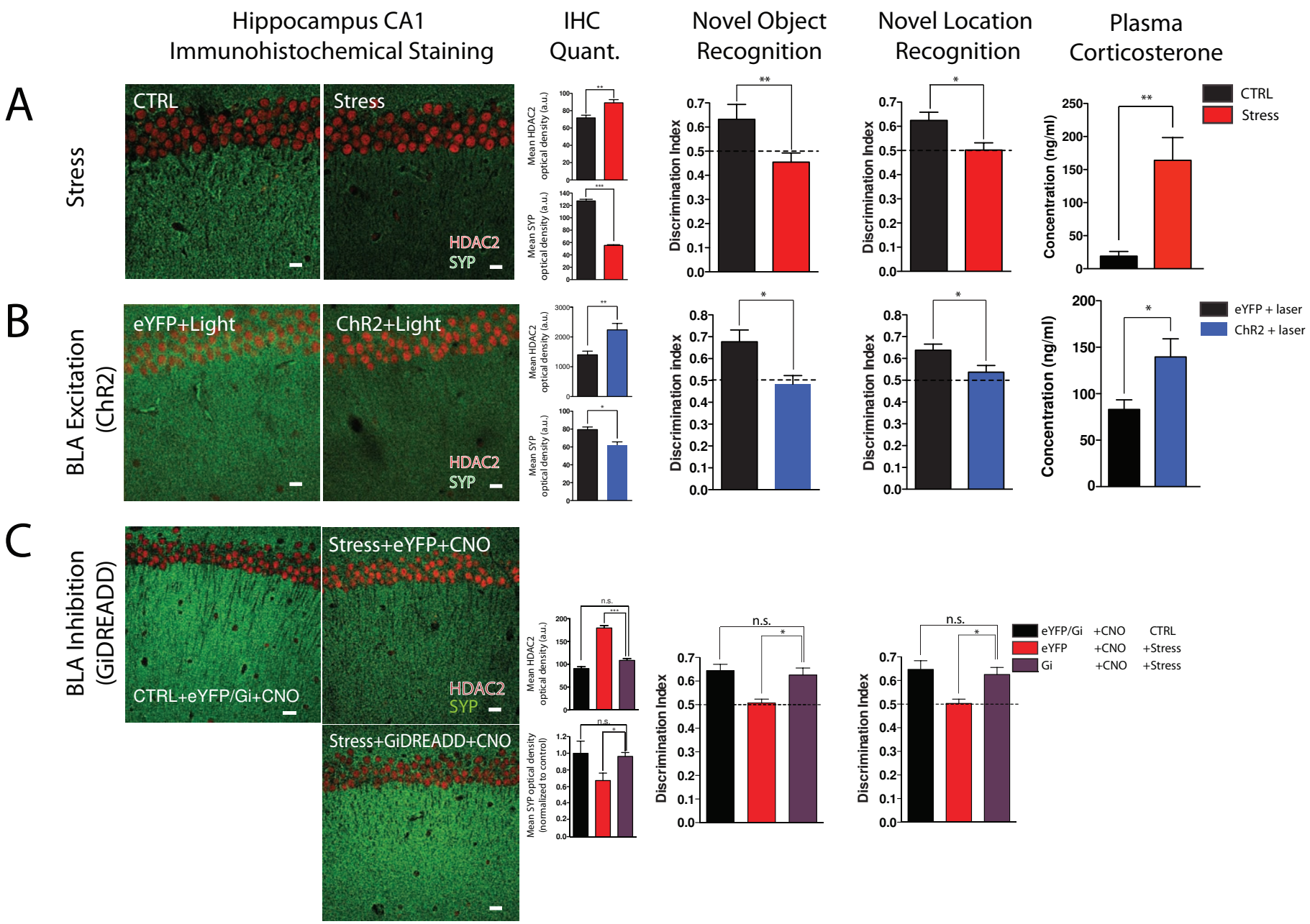
Hippocampus CA1
Immunohistochemical Staining
IHC
Quant.
Novel Object
Recognition
Novel Location
Recognition
Plasma
Corticosterone
A
Stress
CTRL
Stress
HDAC2
SYP
Mean HDAC2 optical density (a.u.)
Mean SYP optical density (a.u.)
Discrimination Index
Concentration (ng/ml)
CTRL
Stress
B
BLA Excitation
(ChR2)
eYFP+Light
ChR2+Light
HDAC2
SYP
eYFP + laser
ChR2 + laser
C
BLA Inhibition
(GiDREADD)
CTRL+eYFP/Gi+CNO
Stress+eYFP+CNO
Stress+GiDREADD+CNO
Mean SYP optical density (normalized to control)
eYFP/Gi +CNO CTRL
eYFP +CNO +Stress
Gi +CNO +Stress

Figure 3

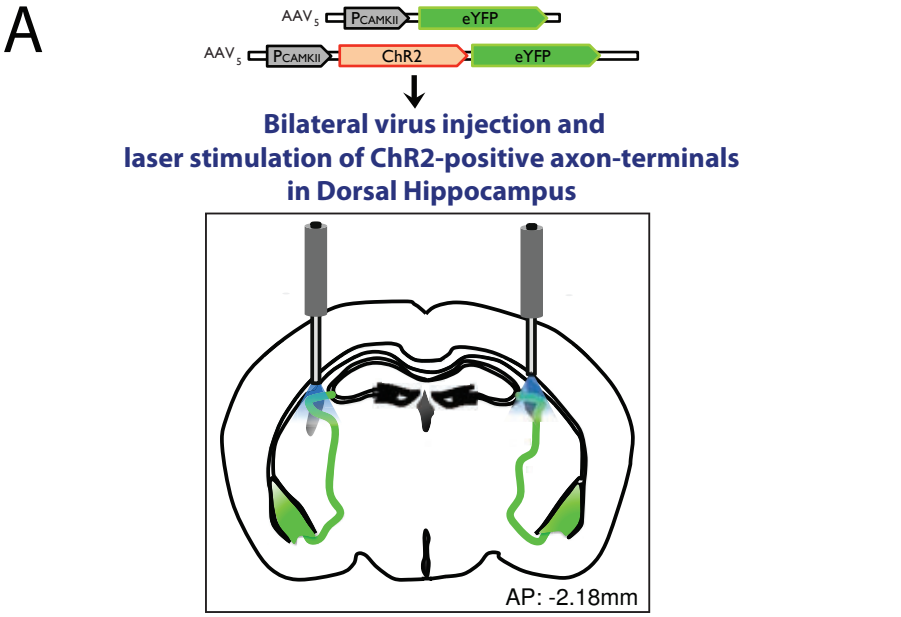
A
AAV5 PCAMKII eYFP
AAV5 PCAMKII ChR2 eYFP
Bilateral virus injection and
laser stimulation of ChR2-positive axon-terminals
in Dorsal Hippocampus
AP: -2.18mm
B
CA1
eYFP-Dorsal
ChR2-Dorsal
HDAC2
SYP
Mean HDAC2 optical density (a.u.)
Mean SYP optical density (a.u.)
C
Novel Object Recognition
Novel Object Location
Discrimination index
D
Plasma
Corticosterone
Concentration (ng/ml)
n.s.
eYFP cage control
eYFP + laser
ChR2 + laser

Figure 4

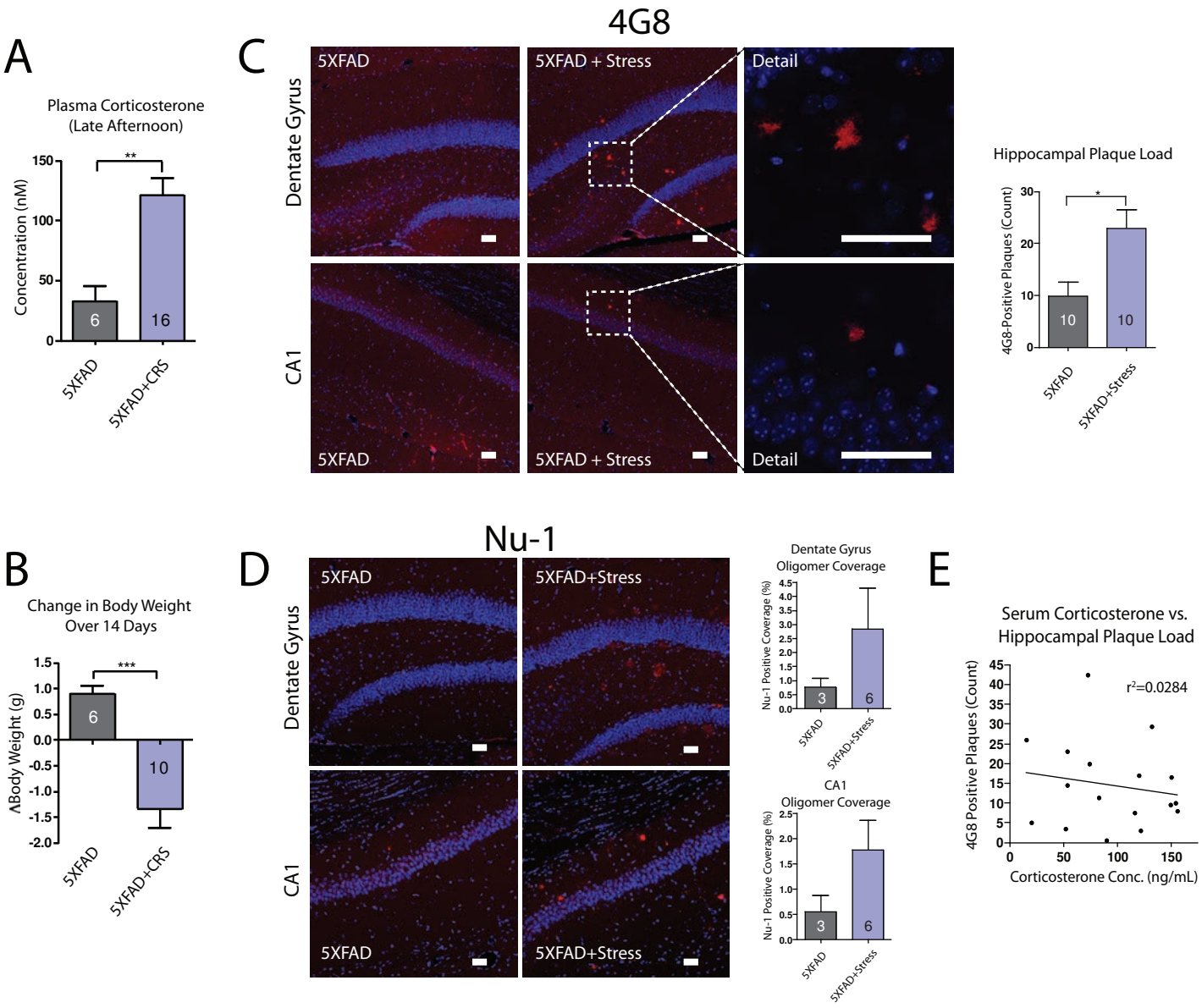
A
Plasma Corticosterone
(Late Afternoon)
Concentration (nM)
150
100
50
0
**
6
16
5XFAD
5XFAD+CRS
B
Change in Body Weight
Over 14 Days
ΔBody Weight (g)
1.5
1.0
0.5
0.0
-0.5
-1.0
-1.5
-2.0
***
6
10
5XFAD
5XFAD+CRS
C
4G8
Dentate Gyrus
CA1
5XFAD
5XFAD + Stress
Detail
5XFAD
5XFAD + Stress
Detail
Hippocampal Plaque Load
4G8-Positive Plaques (Count)
30
20
10
0
*
10
10
5XFAD
5XFAD+Stress
D
Nu-1
Dentate Gyrus
CA1
5XFAD
5XFAD+Stress
5XFAD
5XFAD+Stress
Dentate Gyrus
Oligomer Coverage
Nu-1 Positive Coverage (%)
4.5
4.0
3.5
3.0
2.5
2.0
1.5
1.0
0.5
0.0
3
6
5XFAD
5XFAD+Stress
CA1
Oligomer Coverage
Nu-1 Positive Coverage (%)
2.5
2.0
1.5
1.0
0.5
0.0
3
6
5XFAD
5XFAD+Stress
E
Serum Corticosterone vs.
Hippocampal Plaque Load
4G8 Positive Plaques (Count)
45
40
35
30
25
20
15
10
5
0
r²=0.0284
0
50
100
150
Corticosterone Conc. (ng/mL)

Figure 5

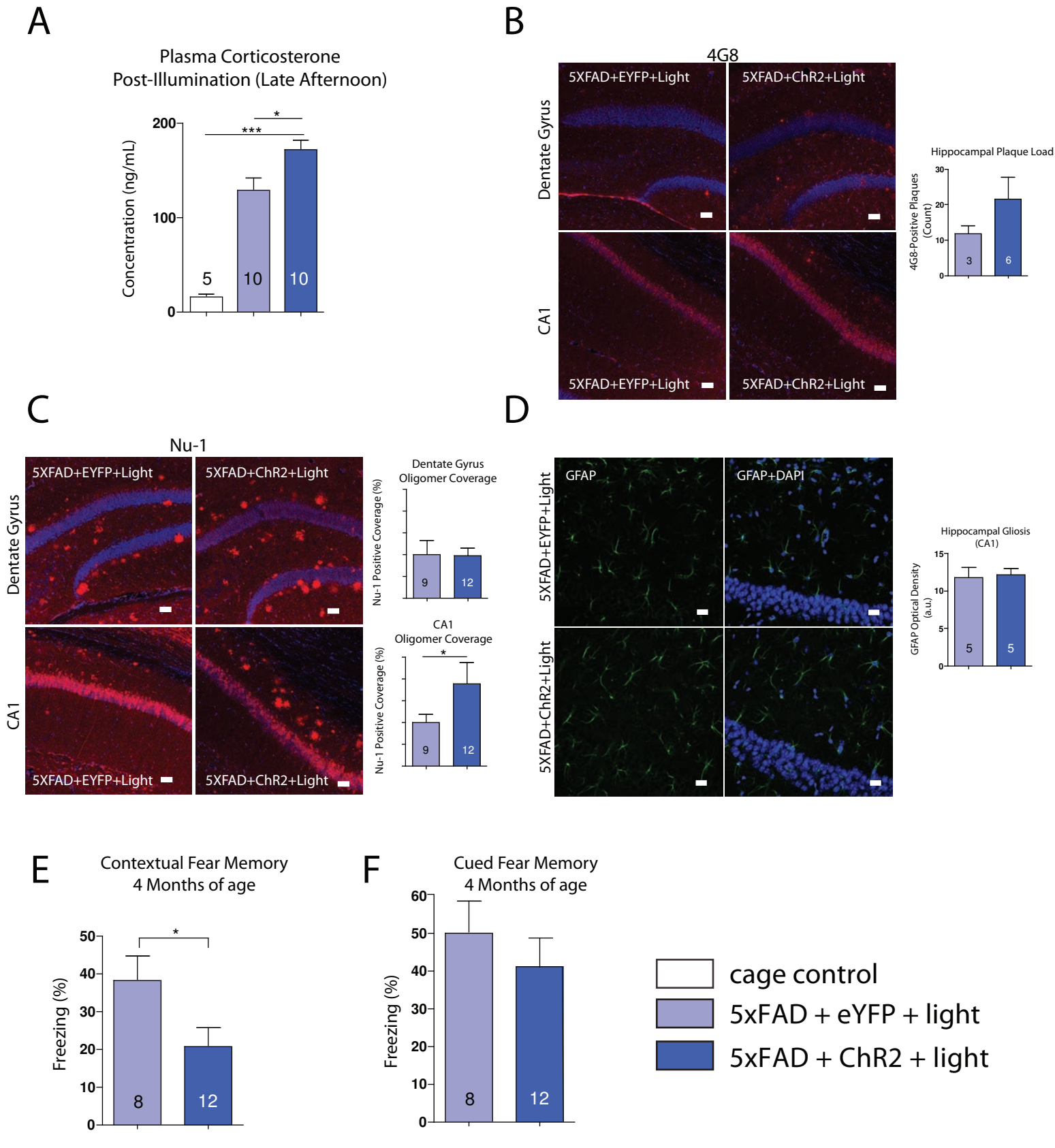
A
Plasma Corticosterone
Post-Illumination (Late Afternoon)
Concentration (ng/mL)
200
100
0
*
***
5
10
10
B
4G8
5XFAD+EYFP+Light
5XFAD+ChR2+Light
Dentate Gyrus
CA1
5XFAD+EYFP+Light
5XFAD+ChR2+Light
Hippocampal Plaque Load
4G8-Positive Plaques (Count)
30
20
10
0
3
6
C
Nu-1
5XFAD+EYFP+Light
5XFAD+ChR2+Light
Dentate Gyrus
CA1
5XFAD+EYFP+Light
5XFAD+ChR2+Light
Dentate Gyrus Oligomer Coverage
Nu-1 Positive Coverage (%)
9
12
CA1 Oligomer Coverage
*
Nu-1 Positive Coverage (%)
9
12
D
GFAP
GFAP+DAPI
5XFAD+EYFP+Light
5XFAD+ChR2+Light
Hippocampal Gliosis (CA1)
GFAP Optical Density (a.u.)
15
10
5
0
5
5
E
Contextual Fear Memory
4 Months of age
Freezing (%)
50
40
30
20
10
0
*
8
12
F
Cued Fear Memory
4 Months of age
Freezing (%)
60
50
40
30
20
10
0
8
12
cage control
5xFAD + eYFP + light
5xFAD + ChR2 + light

Figure 6

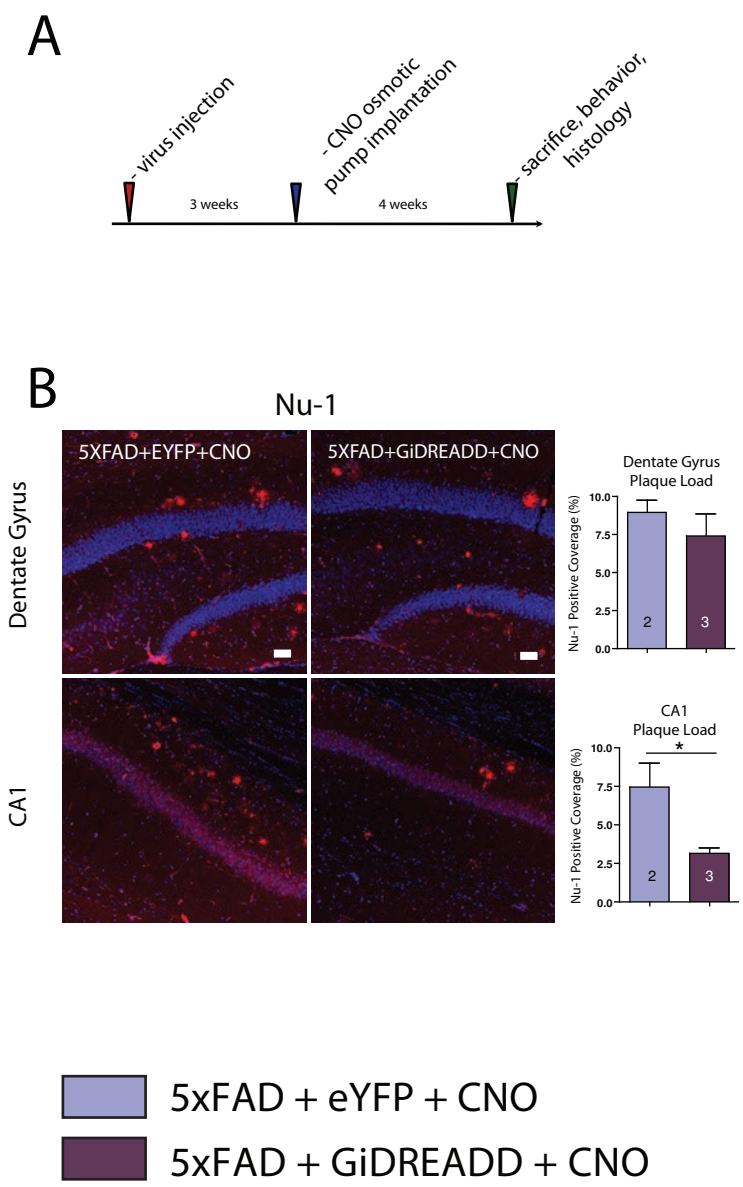
A
virus injection
CNO osmotic pump implantation
sacrifice, behavior, histology
3 weeks
4 weeks
B
Nu-1
5XFAD+EYFP+CNO
5XFAD+GiDREADD+CNO
Dentate Gyrus
CA1
Dentate Gyrus Plaque Load
CA1 Plaque Load
Nu-1 Positive Coverage (%)
*
C
Contextual Fear Memory
7 Months of age
Freezing (%)
D
Cued Fear Memory
7 Months of age
5xFAD + eYFP + CNO
5xFAD + GiDREADD + CNO

Appendix Figure 1

A

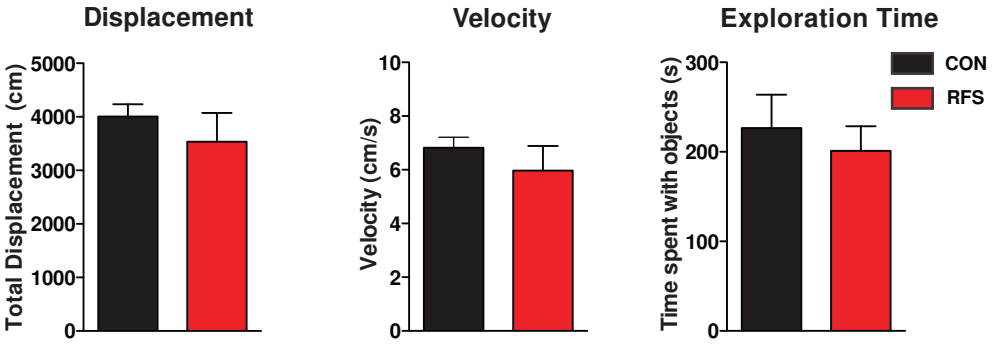

B

Pharmacokinetic Property of CNO	Value	Reference/Derivation
Half-life ($t_{1/2}$) (human)	8.6 hours	Guitton *et al.*, J. Clinical Pharmacology 1999
Clearance (Cl) (human)	45.3 L/hour (40 kg human)	Chang *et al.* 1998, Prog. Neuropsycopharm/Biol. Psych.
Volume of Distribution (V_D) (human)	562 L (40 kg human)	$V\text{-}_D = (Cl * t_{1/2})/\ln 2$
Volume of Distribution (V_D) (mouse)	0.2409 L (30 g mouse)	α body-mass
Clearance (mouse)	0.1352 L/hour (30g mouse)	Kleiber's Law: $q_0 \sim M^{3/4}$
Partition Coefficient	14.05	$V\text{-}_D$/Total Body Water
Effective Concentration	1-10 M	(Ray *et al.*, Science 2011; Armbruster *et al.*, PNAS 2007)

C

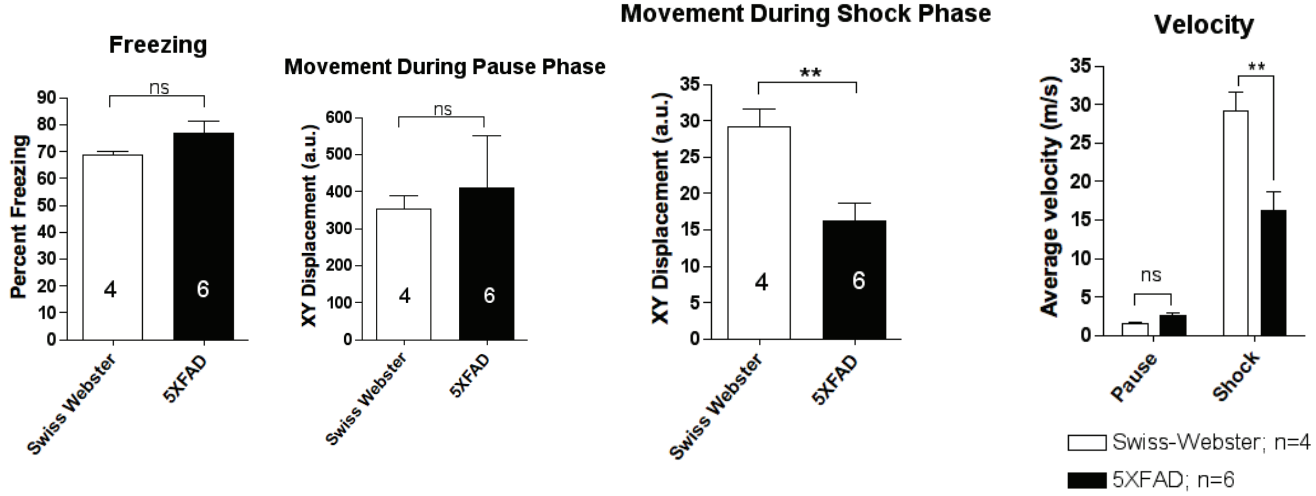

Figure 1: Experimental Paradigms. (**A**) Paradigm for repetitive-footshock treatment in Swiss-Webster mice. Inset shows behavioral testing schedule. (**B**) Optical stimulation paradigm for Swiss-Webster mice undergoing BLA cell body photostimulation. Inset shows behavioral testing schedule. (**C**) Paradigm for intracranial viral injection of eYFP (top) or ChR2-eYFP (bottom) viral constructs, and schematic of location of viral expression, fiber optic implantation, and illumination. (**D**) **1.** G_iDREADD "hM4D(G_i)" generation by ligand binding site mutation (Armbruster, 2007) **2.** Schematic illustrating eYFP or G_iDREADD viral constructs, and territory for viral expression **3.** Upon CNO binding to G_iDREADD, normal G-protein dissociation occurs, leading to activation of G protein-coupled inwardly-rectifying potassium channels (GIRKs) and neuronal inhibition. (**E**) Paradigm for chronic-restraint stress treatment of 5xFAD mice. (**F**) Modified optical stimulation paradigm for 5xFAD mice undergoing BLA cell body photostimulation. Inset shows behavioral testing schedule.

Figure 2: Glutamatergic activity of the basolateral amygdala is both necessary and sufficient to produce the cognitive and molecular effects of chronic stress on hippocampal function. (**A**) **Effects of RFS**: Representative confocal immunohistochemical microscopy demonstrating labelling of synaptophysin and HDAC2 in hippocampus CA1 (leftmost), and densitometric quantification (left; n=4 per group); RFS mice showed no discrimination between old and novel objects or object-locations (discrimination index=0.5 (chance)) in NOR (n=10,16) and NLR (n=10/group); ELISA measurement of mid-afternoon plasma corticosterone demonstrated significant elevation after RFS (n=5/group). (**B**) **ChR2-mediated BLA photostimulation replicates the effects of RFS**: representative confocal microscopy in hippocampus CA1 with densitometric quantification (left, n=5/group) displays reduction in SYP and elevation in HDAC2 similar to that seen after RFS. ChR2/photostimulated mice showed no discrimination between old and novel objects or object-locations (discrimination index=0.5 (chance)) in NOR (n=10,12) and NLR (n=12/group); ELISA measurement of mid-afternoon plasma corticosterone demonstrated significant elevation after RFS

(n=5/group). (**C**) **G_iDREADD-mediated BLA inhibition during RFS prevents the effects of RFS**: representative confocal microscopy in hippocampus CA1 with densitometric quantification (left, n=4,5,6) displays rescue of SYP and HDAC2 after BLA inactivation during RFS by G_iDREADD/CNO treatment. Both novel-object and novel-location discrimination abilities are rescued in RFS mice by G_iDREADD/CNO treatment - NOR (n= 16, 15, 7) and NLR (n=10, 10 and 7).**Scale bar: 20 μm. *P≤0.05; ***P≤0.001, values are mean±s.e.m.**

Figure 3: Photostimulation of BLA afferent axon terminals in the hippocampus CA3 is sufficient to reproduce the cognitive and molecular effects of chronic stress on hippocampal function. (**A**) Constructs for eYFP-control (top) or ChR2-eYFP (bottom) virus used in bilateral intra-BLA injection; Paradigm demonstrating location of viral expression, optical fiber implantation, and illumination. (**B**) Representative confocal immunohistochemical microscopy demonstrating labelling of synaptophysin and HDAC2 in hippocampus CA1, and densitometric quantification (right; n=5 per group)(**C**) Cognitive testing using hippocampus-dependent paradigms demonstrated that ChR2/terminal photostimulated mice showed no discrimination between old and novel objects or object-locations (Discrimination index=0.5 (chance)) in NOR (n=16,10) and NLR (n=16/10). (**D**) ELISA measurement of mid-afternoon plasma corticosterone (n=5/group). **Scale bar: 20 μm. *P≤0.05; ***P≤0.001, values are mean±s.e.m.**

Figure 4: Chronic restraint stress (CRS) worsens disease progression in the 5XFAD murine model of AD. (**A**) ELISA measurement of mid-afternoon plasma corticosterone after 1 session of CRS or control treatment. (**B**) Change in body weight after 14 daily sessions of CRS or control treatment. (**C**) Representative confocal microscopy demonstrating increased overall hippocampal Aβ plaque burden by 4G8 antibody staining, including digital-zoom image showing individual plaques (left panels, representative images; right panel, quantification by counts under epifluorescence). (**D**) Representative confocal microscopy

demonstrating increased overall hippocampal Aβ oligomer coverage by Nu-1 antibody (left panels, representative images; right panels, quantification). (**E**) Plasma corticosterone concentration following a single stress-treatment does not correlate with hippocampal plaque load (pearson correlation coefficient = 0.0284) **Scale bar: 50 uM. * p<0.05; ** p< 0.01, ***p<0.001. Numbers within bars represent sample size.**

Figure 5: Chronic BLA photoactivation exacerbates AD-like pathology and cognitive impairment in 4 month-old 5XFAD mice. (**A**) ELISA measurement of mid-afternoon plasma corticosterone in undisturbed cage controls, or after 1 session of BLA photostimulation of eYFP or ChR2-injected mice. (**B**) Representative confocal microscopy demonstrating increased overall hippocampal Aβ plaque burden by 4G8 antibody staining, including quantification by counts under epifluorescence. (**C**) Representative confocal microscopy demonstrating increased Aβ oligomer coverage by Nu-1 antibody staining in the hippocampus CA1 (rightmost panels – quantification by binary intensity-thresholded percent area). (**D**) Representative confocal microscopy demonstrating no change in GFAP intensity in the hippocampus CA1 (rightmost panels – quantification by overall intensity. (**E, F**) 14 days of BLA photostimulation leads to a deficit in contextual fear memory (**E**), but no difference in cued fear memory (by presentation of the stimulus tone)(**F**). **Scale bar: 50 uM * p<0.05; ** p< 0.01, ***p<0.001. Numbers within bars represent sample size.**

Figure 6: Chronic BLA inactivation by G_iDREADD reduces AD-like pathology and may improve cognition in 7 month-old 5XFAD mice. A. Experimental paradigm for genetic-pharmacological BLA inactivation by G_iDREADD (**B**) Representative confocal microscopy demonstrating reduced hippocampal Aβ oligomers in hippocampus CA1 by Nu-1 staining (right panels, quantification by binary intensity-thresholded percent area). (**C,D**) 4 weeks of BLA inactivation may produce a slight improvement in contextual fear memory (**C,** not significant), but did not lead to a change in fear memory cued by presentation of the

stimulus tone (**D**). **Scale bar: 50 uM * p<0.05; ** p< 0.01, ***p<0.001. Numbers within bars represent sample size.**

Appendix Figure 1: (**A**) Computerized tracking during NOR testing demonstrates no difference in various control behavioral measures between RFS and context-only (control) treated mice (n=10,16). (**B**) Table of pharmacokinetic parameters used to calculate approximate tissue-concentrations of CNO. (**C**) Computerized tracking demonstrates that Swiss-Webster and 5xFAD mice respond differently to shocks in the RFS paradigm, but freeze identically. These results were considered sufficient to justify adjusting the stress paradigm in 5xFAD mice. *** p<0.05; ** p< 0.01, ***p<0.001. Numbers within bars represent sample size.**